Table I. Formats of the tissue microarray.

Tissue microarray[a]	Organ	Specificity
MC5003	Multiple	High-density multiple organ tumor and normal tissue microarray, containing 18 types of tumor (20 spots/type) and normal controls (5 spots/type)
BRM961	Breast	Breast carcinoma metastatic tissue microarray, containing 96 spots of breast cancer, with 72 matched metastatic breast cancer (in lymph nodes) and 24 normal tissue
BR1503	Breast	Breast carcinoma tissue microarray (including TNM and pathology grade, with IHC results of HER2, ER, PR, P53 and Ki-67), containing 6 spots of normal tissue, 6 fibroadenoma, 4 cystosarcoma phyllodes, 14 intraductal carcinoma, 120 invasive ductal carcinoma
TH807	Thyroid	Thyroid disease spectrum tissue microarray, 10 spots of each types (papillary carcinoma, follicular carcinoma, metastatic carcinoma, adenoma, goiter, thyroiditis, cancer adjacent normal and normal tissue)
CR602	Uterine cervix	Uterine cervical disease spectrum tissue microarray, containing 30 spots of uterine cervix tumor, 10 spots of CIN, 10 spots of inflammation and 10 adjacent normal tissue
TE803	Testis	Testis disease spectrum (testicular cancer progression) tissue microarray, containing 26 spots of seminoma, 12 embryonal carcinoma, 10 yolk sac tumor, 7 teratoma, 4 tuberculosis, 6 atrophy, 10 adjacent normal tissue and 5 normal tissue

[a]Tissue microarrays were chosen from the lineups of US Biomax products. Product ID is indicated.

FAM107A has been regarded as a candidate of tumor suppressor gene (TSG) because of its decreased expression in cancer and because of the fact that introduction of FAM107A suppresses cancer cell proliferation and induces apoptosis (7,10-13). In contrast, it was recently reported that FAM107A is highly expressed in the invasive component of gliomas and that it drives tumor invasion by functioning as a new cytoskeletal crosslinker that regulates focal adhesion dynamics and cell movement (14,15). Consequently, the physiological role and function of FAM107A as a TSG remain controversial.

In humans, FAM107B protein is encoded by the gene on chromosome 10p13, sharing 65% sequence similarity with FAM107A in their N-terminal DUF1151 regions. We previously investigated histopathological localization and functions of FAM107B in gastrointestinal cancers, and designated it as heat-shock-inducible tumor small protein (HITS) (16) based on its unique expression pattern and biological properties in cancer cells and its low molecular weight (18 kDa) among a family of heat-shock proteins (HSPs) (17-19). Similar to FAM107A, HITS expression is decreased or absent in gastric and colorectal cancers; moreover, it inhibits tumor cell proliferation *in vitro* (16), which contrasts with previously described oncogenic activities of other HSPs such as HSP70 and HSP90 (20-24).

In this study, we performed immunohistochemical examination of HITS expression in cancer tissues of the multiple organs spotted on tissue microarrays that include clinical and histopathological information of the respective tumor samples. Consistent with the hypothesis that HITS is a tumor suppressor protein in gastrointestinal cancer (16), our current study demonstrated that loss of HITS expression is commonly observed in cancers of multiple organs and involved in tumor proliferation.

Materials and methods

Tissue microarrays. Several types of human tissue microarrays including normal, malignant, and metastatic formats (US Biomax, Inc., Rockville, MD) were used to examine HITS expression in cancer and to compare the results with clinical and histopathologic characteristics of the tumors (Table I). The high-density multiple organ tumor and normal tissue microarray (MC5003) was used for the initial screening of HITS expression. This microarray includes 18 types of tumor (20 cases/each tumor type) and normal tissues (5 cases/each organ) with TNM classification and pathology grades of the tumors. According to results of HITS expression in MC5003 tissue microarray and statistical analysis, additional analysis of individual organs was used with the following tissues microarrays. BR1503 is a breast cancer tissue microarray that includes TNM classification and pathology grades of the respective tumor spots and the levels of immunohistochemical expression of human epidermal growth factor receptor 2 (HER2), estrogen receptor (ER), progesterone receptor (PR), p53 and Ki-67. BRM961 is a breast cancer tissue microarray including the spots of primary and matched metastatic tumors in lymph nodes and adjacent normal breast tissues. TH807 includes tissue spots of various thyroid diseases. CR602 includes the tissue spots of uterine cervical diseases [cervical cancer, cervical intraepithelial neoplasia (CIN), inflammation] and adjacent normal tissues, and TE803 includes those of testis diseases (testicular benign and malignant tumors).

Antibodies. To generate a polyclonal anti-human HITS antibody, rabbits were immunized with keyhole limpet hemocyanin (KLH)-conjugated polypeptides (MAEPDYIEDDNPE) as an antigen (16). The antibody was purified from the anti-serum using affinity chromatography against the same polypeptides

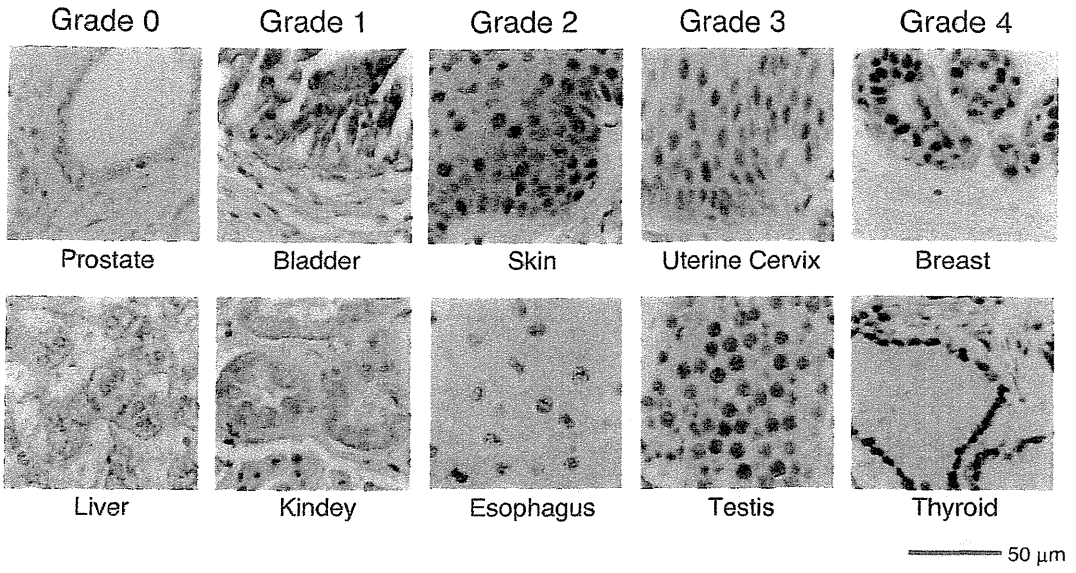

Figure 1. Scoring of HITS expression. Immunohistochemical evaluation of HITS expression was classified into grades 0-4 according to its signal intensity and nuclear localization. Representative findings of the indicated scores of HITS expression in the respective normal tissues are shown.

cross-linked to agarose beads, and verified its specificity by flow cytometry of immunostaining and western blot analysis. Antibodies to β-actin (Santa Cruz Biotechnology, Santa Cruz, CA), proliferating cell nuclear antigen (PCNA) and survivin (Dako A/S, Glostrup, Denmark) were purchased.

Immunohistochemistry. Expression and localization of HITS, PCNA and survivin in paraffin sections of tissues and microarrays were examined using immunohistochemical staining, as conducted in a previous study (25). Representative paraffin sections and tissue microarrays placed on silanized slides were treated by microwaving in the citrate buffer to unmask antigens. Then they were incubated with 0.3% H_2O_2 in methanol and with 10% normal goat serum for blocking endogenous peroxidase activity and nonspecific antibody binding. The pretreated sections were incubated with the respective antibodies (1:500 dilution each) overnight at 4˚C with subsequent serial incubation with the biotinylated goat anti-rabbit IgG (Vector Laboratories Inc., Burlingame, CA) and standard avidin-biotin-peroxidase complex (ABC). Cell nuclei were counterstained with hematoxylin.

Scores for HITS expression and statistical analysis. We assigned grades 0-4 to microscopic evaluation of HITS expression in tissues according to the signal intensity and nuclear localization of HITS (Fig. 1). Grade 0, no staining in cytoplasm and nucleus; grade 1, borderline cytoplasmic staining but no apparent nuclear localization; grade 2, weak nuclear staining; grade 3, moderate nuclear staining; grade 4, strong nuclear staining.

Scores of HITS grading in the respective groups of tissue specimens were expressed as means ± standard deviation (SD). The mean scores of HITS expression of the two groups were compared using two-sided Mann-Whitney U tests. For comparison of the scores of more than two groups, the significance of differences among the data was determined using one-way ANOVA followed by Scheffe's F post hoc test. Correlation between scores of HITS expression and the clinical and pathological parameters of the tumors was determined using the nonparametric Spearman's rank correlation analysis. Values of $P<0.05$ were considered significant.

In breast cancer, desmoplastic reaction, also called reactive fibrosis, is characterized by mobilization of fibroblasts and deposition of abundant collagen as a stromal response to an invasive carcinoma. The HITS expression scores for breast cancers with and without desmoplastic stromal reaction were compared statistically.

In vivo tumorigenicity assays. We previously established a human uterine cervical-cancer-derived HeLa Tet-On advanced cell line (Clontech Laboratories, Inc., Mountain View, CA) transduced with a mock or Tet-inducible HITS gene (16). Cells ($1x10^6$) of each HeLa cell line were inoculated subcutaneously to two opposite sites of flank in each Scid mouse (n=14; Charles River Laboratories Japan Inc., Yokohama, Japan). These mice were divided into two groups and treated or not treated with doxycycline (1.5 mg/ml; Clontech Laboratories Inc.) dissolved in drinking water in light-protected bottles, respectively, for 8 weeks. Following treatment, all mice were euthanized. Tumors removed from mice were weighed and fixed in neutral-buffered 10% formalin and embedded in paraffin for histopathologic and immunohistochemical examination. Tumor formation in mice with (n=7) or without (n=7) doxycycline administration was expressed as average weight ± SD. The statistically significant difference in tumor formation between the groups was determined using a two-sided Mann-Whitney U test, for which $P<0.05$ was considered significant. We repeated this experiment twice to confirm reproducibility. The animal study was conducted according to the Guidelines for Experimental Animals at Kanazawa Medical University and the National Guidelines for Animal Usage (http://www.lifescience.mext.go.jp/policies) in Japan.

Results

Screening for the expression of HITS in multiple tissues. The high-density multiple organ tumor and normal tissue array

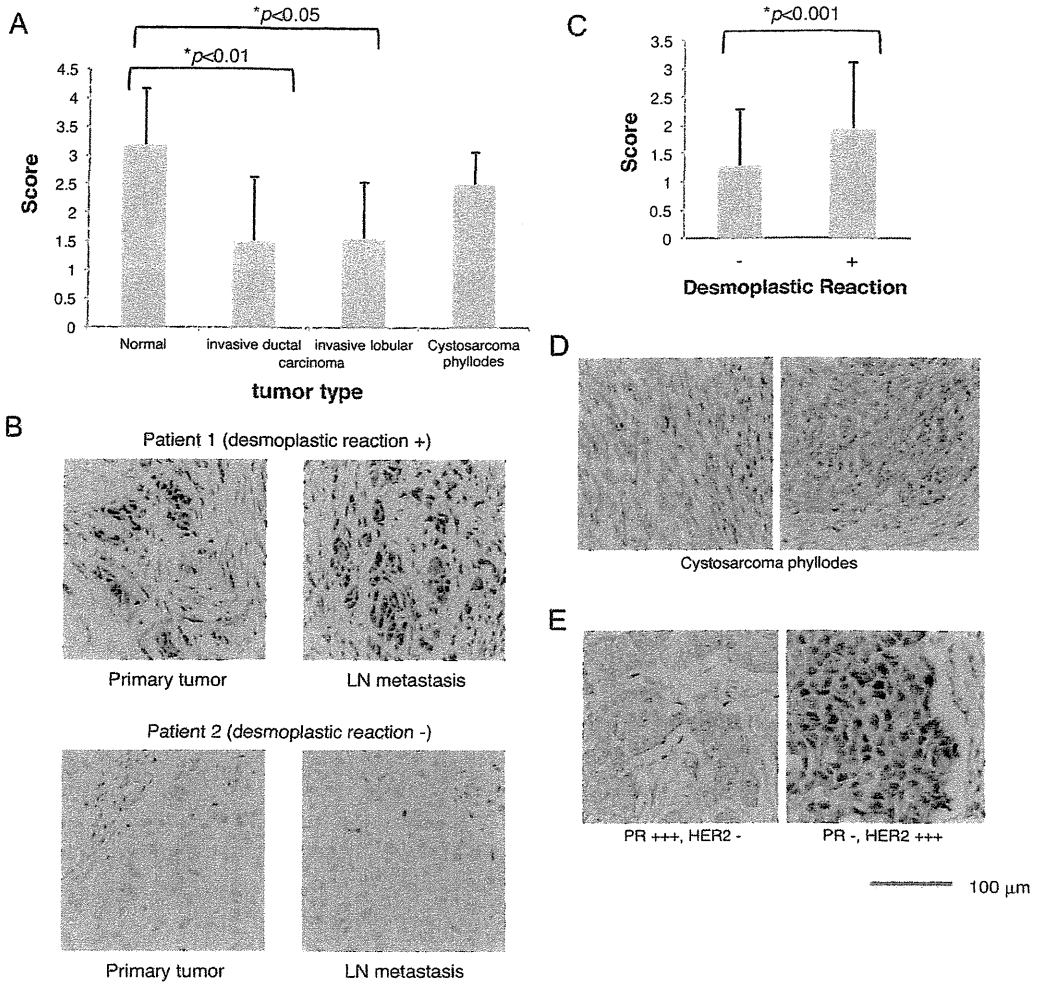

Figure 2. HITS expression in breast tumors. (A) Scores of HITS expression in tissue microarrays MC5003, BR1503 and BRM961 are summed up in normal breast tissues (n=23), invasive ductal carcinoma (n=177), invasive lobular carcinoma (n=7) and cystosarcoma phyllodes (n=4), respectively, and are expressed as means ± SD and compared by Scheffe's F post hoc test. (B) HITS expression was compared between the primary tumor and lymph node metastasis in the patient 1 or 2 with or without desmoplastic reaction, respectively. (C) Breast cancers were classified into two groups with (n=67) and without (n=119) desmoplastic reaction. The scores of HITS expression of the two groups were compared. Statistical analysis was performed using two-sided Mann-Whitney U test. Representative staining with (D) IHC of HITS in cystosarcoma phyllodes and (E) PR(+++), HER2(-) or PR(-), HER2(+++) invasive ductal carcinoma is shown. *Denotes a statistically significant effect ($p<0.05$, bracket).

(MC5003) including tumors of 18 types along with corresponding normal tissues was used for immunohistochemical screening for the expression of HITS. Scores of HITS expression in normal (n=5) and cancer tissues (n=20) in each organ are added up separately, expressed as mean ± SD, and compared statistically using the Mann-Whitney U test. Despite the small number of samples in each group, lower expression of HITS in tumor tissues than their normal counterparts was frequent to a significant degree in cancers of the thyroid, breast, colon, and uterine cervix (Table II). Scores of HITS expression in cancer tissues seemed lower than their normal counterparts in the lung, stomach, and testis, although no statistically significant differences were found among them. In contrast, in the tumors of the liver, pancreas, ovary, and urinary tracts including the kidney, bladder, and prostate, scores of HITS expression in cancer tissues seemed slightly higher than those in the corresponding normal tissues, although the intensity of HITS expression in these organs was very low, even in normal tissues (Table II and Fig. 1).

Through screening of the MC5003 tissue array, we selected four organs of the breast, thyroid, testis and uterine cervix for the next step of investigation of detailed pathological analysis and statistical analysis using cancer tissue arrays of the respective organs to explore HITS expression in the tumors (Table I).

HITS expression in breast cancer. Because HITS expression was high in normal breast tissues (Table II and Fig. 1), average scores of HITS expression summed up in the normal tissues spotted on the three tissue-microarrays MC5003, BR1503 and BRM961 were 3.17±0.98. The mean score of HITS expression in cancer tissues was 1.50±1.08, which was significantly lower than in normal tissues ($p<0.001$). Decreased HITS expression was common to the two representative histological types of breast cancers, invasive ductal and lobular carcinomas (Fig. 2A). Comparison of cancers with different stromal reactions revealed that the breast cancers associated with desmoplastic reaction exhibited significantly higher HITS expression than those without this stromal reaction (Fig. 2B and C). Cystosarcoma

Table II. Immunohistochemical screening for the expression of HITS in multiple organs and tissues.

	Normal[a] (n=5)	Cancer[a] (n=20)	P-value[b]
Brain	2.20±1.30	2.70±1.34	0.43
Head and neck	2.80±1.10	2.67±0.84	0.61
Thyroid	3.80±0.45	1.30±0.73	<0.01
Lung	3.00±1.00	2.25±1.12	0.18
Breast	4.00±0.00	2.40±1.19	<0.01
Esophagus	2.20±1.30	1.55±1.10	0.28
Stomach	2.33±1.15	1.31±1.08	0.13
Colon	3.20±0.45	1.42±0.69	<0.01
Liver	0.60±0.55	0.75±0.44	0.51
Pancreas	1.20±0.45	1.58±0.96	0.51
Uterus	1.60±1.34	1.84±1.12	0.42
Uterine cervix	3.80±0.45	1.68±0.89	<0.01
Ovary	1.60±1.14	1.80±1.01	0.80
Kidney	0.80±0.45	1.35±1.42	0.64
Bladder	2.00±1.41	2.75±1.12	0.24
Prostate	0.80±0.84	1.63±1.21	0.15
Testis	3.60±0.55	2.21±1.23	0.06
Soft tissue	3.40±0.55	3.35±0.88	0.82
Skin	3.00±0.00	2.40±1.18	0.29
Lymph node	2.20±0.84	1.70±0.92	0.23

[a]HITS expression scores of normal (n=5) and cancer tissues (n=20) in each organ are added separately (tissue array: MC5003). Data are the mean ± SD. [b]Scores are compared using the Mann-Whitney U test; P<0.05 was considered statistically significant.

Table III. Expression of HITS for breast cancer.

Parameter	HITS mean ± SD (n)	rs	P-value
TNM stage[a]		-0.19	0.01
I	1.71±0.91 (14)		
IIa	1.68±1.15 (92)		
IIb	1.27±1.07 (45)		
IIIa	1.47±1.22 (19)		
IIIb	1.07±0.80 (15)		
T[a]		-0.23	<0.01
1	1.71±0.91 (14)		
2	1.67±1.17 (126)		
3	1.03±0.87 (31)		
4	1.07±0.55 (15)		
N[a]		-0.05	0.48
0	1.55±1.10 (132)		
1	1.34±1.09 (38)		
2,3	1.63±1.20 (16)		
ER[b]		0.02	0.82
- ~ +	1.43±1.04 (88)		
++ ~ +++	1.37±1.02 (43)		
PR[b]		-0.22	<0.05
- ~ +	1.55±1.02 (87)		
++ ~ +++	1.14±1.00 (44)		
TP53[b]		-0.06	0.47
- ~ +	1.45±1.08 (85)		
++ ~ +++	1.34±0.93 (46)		
HER2[b]		0.23	<0.01
- ~ +	1.27±1.20 (41)		
++ ~ +++	1.48±0.94 (90)		
Ki-67[b]		0.33	<0.001
- ~ +	1.27±1.28 (30)		
++ ~ +++	1.46±0.94 (102)		
Histological grade[c]		0.006	0.93
1	2.17±1.17 (6)		
2	1.38±1.07 (134)		
3	1.68±1.09 (31)		
Age[c]		0.13	0.07
<49	1.36±1.08 (105)		
>50	1.64±1.08 (90)		

[a]The relation between tumor progression and HITS expression was examined according to the TNM classification and investigated using nonparametric Spearman rank correlation analysis (tissue arrays: MC5003, BR1503, BRM961). [b]Correlation between HITS expression and pathological parameters was investigated: HITS expression scores were collected in each grade of IHC results (-, +, ++, +++) of HER2, ER, PR, P53 and Ki-67 described in tissue array BR1503. Data were statistically compared using the nonparametric Spearman's rank correlation analysis. Scores of HITS expression were summed up separately in - ~ + or ++ ~ +++ of HER2, ER, PR, P53 and Ki-67 expression, and are shown as means ± SD (tissue array: BR1503). [c]The relation to histological grade and age was investigated. Histological grades 1-3 in pathology diagnosis are, respectively, equivalent to well differentiated, moderately differentiated, and poorly differentiated (The American Joint Commission on Cancer; http://www.cancerstaging.org/). HITS expression scores in each grade or generation and statistical results with the nonparametric Spearman's rank correlation analysis are shown (tissue arrays: MC5003, BR1503, BRM961).

phyllodes is a rare, usually large, fast growing breast tumor that arises from periductal cells of the breast; it is regarded as a borderline malignancy (26). This tumor showed an intermediate score of HITS expression between normal and carcinoma tissues (Fig. 2A and D).

The relation between tumor progression and HITS expression was examined according to the TNM classification. In the results of statistical analysis presented in Table III, the HITS expression scores were lower in accordance with advances in the TNM stages of tumors (rs=-0.19, p=0.01). They were inversely correlated with the T-value (primary tumors) but not with the N-value (lymph node metastasis). To support this, the intensity of HITS expression showed no difference between the primary and metastatic lymph node tumors in the same patients (1.37±1.17 and 1.23±0.94, respectively, p=0.40) (Fig. 2B). No relation to the histological grade of tumor differentiation was found (Table III).

Although the most important prognostic factors are the tumor size, histological grade and lymph node stage (27), the importance of several molecular markers in breast cancer has been of considerable interest recently, not only as prognostic markers, but also as predictors of response to therapy (28). For further analysis of correlation between HITS expression and other pathological parameters, we exploited the tissue microarray BR1503, which includes data of immunohistochemical expression of HER2, ER, PR, p53 and Ki-67 in addition to those of TNM stages and

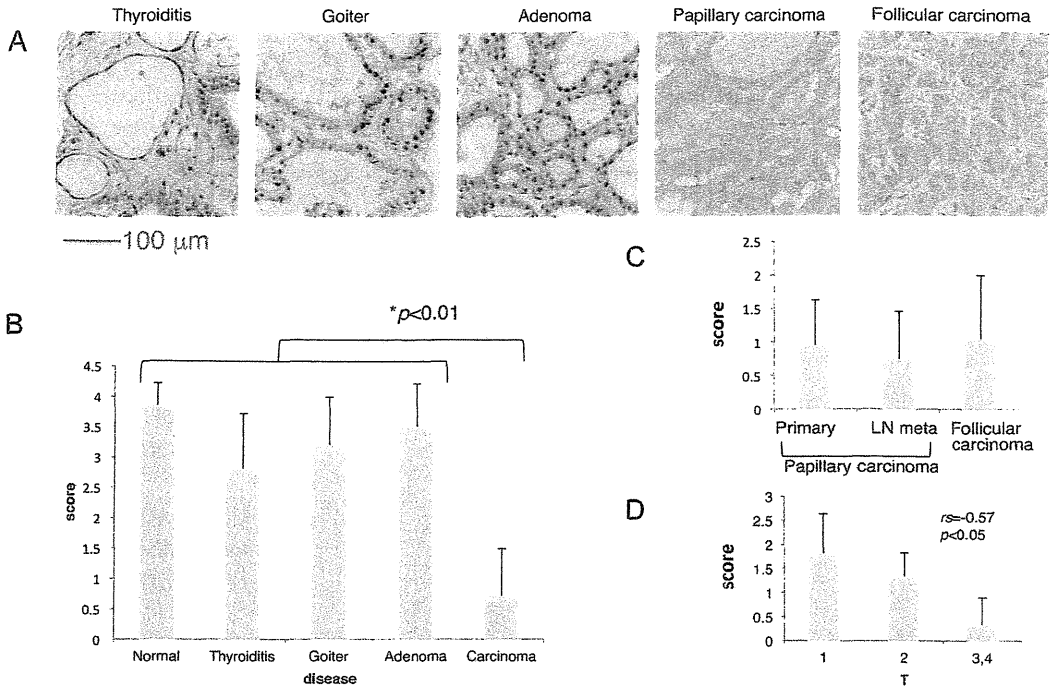

Figure 3. HITS expression in thyroid diseases. (A) Representative findings of HITS expression in the different thyroid diseases. (B) Scores of HITS expression in the tissue microarrays MC5003 and TH807 are summed up in normal thyroid tissues (n=24), thyroiditis (n=10), goiter (n=10), adenoma (n=10) and carcinoma (n=41), respectively, and are shown as the mean ± SD. Statistical analysis using Scheffe's F post hoc test indicates a significant difference in HITS expression scores between carcinoma and normal or benign thyroid diseases. (C) Comparison of HITS expression between the primary tumors and lymph node metastasis of papillary carcinoma (n=11) and follicular carcinoma (n=10) in the tissue array TH807 are shown. (D) Inverse correlation between HITS expression scores and the T-value of the TNM grading were revealed by nonparametric Spearman's rank correlation analysis (rs=-0.57, p<.05). The numbers of samples were T1 (n=5), T2 (n=12) and T3 or 4 (n=3). *Denotes a statistically significant effect (p<.05, bracket).

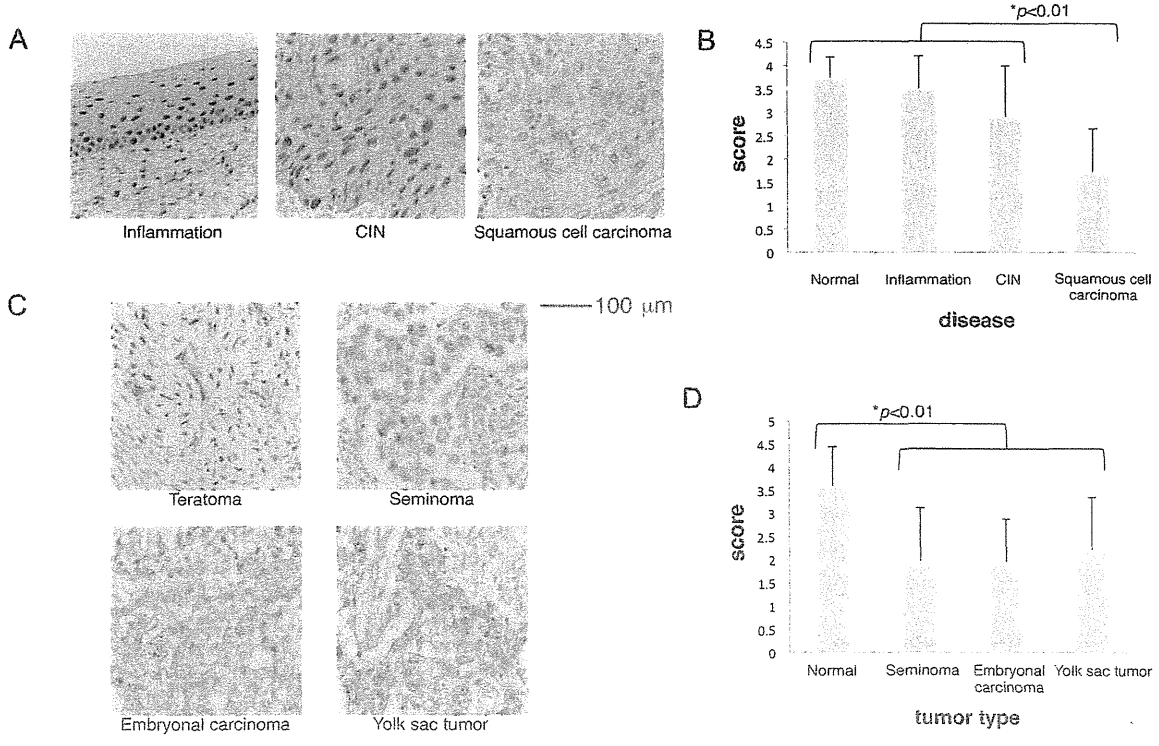

Figure 4. HITS expression in the uterine cervical tissues and the testicular tumors. (A) Representative staining patterns of HITS in various cervical diseases. (B) HITS expression scores in normal tissues (n=15), lesions with inflammation (n=10), CIN (n=10) and invasive squamous cell carcinoma (n=49) of the uterine cervix on the tissue microarrays MC5003 and CR602 are shown as the mean ± SD. They are statistically compared using Scheffe's F post hoc test. (C) Representative findings of HITS expression in benign teratoma and malignant tumors of the testis. (D) Scores of HITS expression in normal testis (n=26), seminoma (n=41), embryonal carcinoma (n=16) and yolk sac tumor (n=10) on the tissue microarrays MC5003 and TE803 were compared statistically using Scheffe's F post hoc test. *Denotes a statistically significant effect (p<0.05, bracket).

pathology grade (Table I). Statistical analysis revealed that the score of HITS expression was correlated positively with the expressions of HER2 (rs=0.23, p<0.01) and Ki-67 (rs=0.33, p<0.001), but inversely with PR expression (rs=-0.22, p<0.05) (Table III). For example, the average score of HITS expression in cancers showing PR- and HER2+++ was 2.16±0.99 (n=25), although the score of HITS expression in the two cases with PR+++ and HER2- was grade 0 (p=0.02) (Fig. 2E). Among other pathological parameters, age has been shown to be a prognostic factor: young patients (<35 years) with breast cancer have a poorer prognosis (29). The present study showed an apparent trend in the increase of HITS scores in cancer tissue in accordance with age, although it was not statistically significant (rs=0.13, p=0.07) (Table III). Means of HITS expression scores in normal breast tissues were greater than 3.0 in all generations (data not shown).

HITS expression in the thyroid, uterine cervical and testicular diseases. In analysis of the thyroid disease tissue microarray (TH807), the HITS expression intensity clearly distinguished thyroid cancer (papillary and follicular carcinomas) from normal tissue, thyroiditis, diffuse goiter, and adenoma (Fig. 3A and B). Consistent with the results obtained for breast cancer, the HITS expression level was similar in primary tumor and lymph node metastasis in the same patients, but inversely correlated with the T-values of TNM grading (Fig. 3C and D).

Regarding analysis of the uterine cervical disease tissue microarray (CR602), HITS expression was found in cervical epithelial cell nuclei in inflammation and CIN, but it was markedly decreased in invasive squamous cell carcinoma (Fig. 4A and B). Infection of human papilloma virus (HPV) is known as an inducer of cervical cancers because of strong causal relations between HPV infection, CIN and invasive carcinoma (30). Because some lesions among those of CIN progress to invasive cancer in 10 to 20 years (31), our results suggest that HITS expression is lost during the progression of CIN toward invasive carcinoma.

Analysis of the testis disease tissue microarray (TE803) showed that, similar to normal breast, thyroid and uterine cervix tissues, HITS expression was high in normal testis (average score >3.5) (Table II, Figs. 1 and 4D). Tumors of the testis, including germ cell tumors (seminoma) and embryonic tumors (embryonal carcinoma and yolk sac tumor), showed significantly lower expression of HITS than either normal testis or benign teratoma (Fig. 4C and D). No significant difference was found in expression levels of HITS between seminoma and non-seminomatous tumors (embryonal carcinoma and yolk sac tumor).

Inducible expression of HITS in vivo reduces tumor size. Based on the immunohistochemical analysis of breast and thyroid cancer tissue microarrays showing that intensity of HITS expression is inversely correlated with the T-value of TNM grading, i.e. primary tumor size, we hypothesized that tumor proliferation might be inhibited by ectopic or forced expression of HITS, which functions as a tumor suppressor protein. Previously, we reported that tetracycline-inducible expression (Tet-ON) of HITS in cancer cells diminished proliferation in response to growth factors such as epidermal growth factor, fibroblast growth factor and fetal calf serum (16). To investigate the role of HITS in tumor proliferation *in vivo*, HITS-transduced and mock-transduced human cervical cancer HeLa cells were transplanted subcutaneously in the flank of Scid mice. Then their tumor formation status was observed for 8 weeks with or without induction of HITS by doxycycline administration in drinking water. As portrayed in Fig. 5A, all mock-transduced cells developed tumors, whereas the Tet-inducible HITS-transduced cells generated tumors in the absence of HITS induction, indicating the suppressive role of HITS for tumor growth. The HITS-induced tumors, although very rarely generated (only one out of seven) and small (Fig. 5A), were processed for histological examination. Regarding pathological examination of the tumors, HITS-induced tumors showed no morphologically distinct gross or microscopic differences except for tumor size (Fig. 5A and B). Immunohistochemical staining of PCNA and survivin showed no apparent difference in intensities between tumors with and without HITS induction, although the area of positively stained cells surrounding central necrosis was much less in HITS-induced tumors than in non-induced tumors, which might reflect the minimal size of tumor formation (Fig. 5C).

Discussion

In this study, we clarified that loss of HITS expression in cancer is common among organs in which the expression level of HITS was high in respective normal tissues. Statistical analysis of data obtained from tissue microarray examination revealed the relevance of HITS expression scores to several pathological parameters, especially to primary tumor size (Table III and Fig. 3D). Forced induction of HITS in cancer cells inhibited the proliferation of tumor xenografts in rodents. These results suggest that HITS might be a tumor suppressor in breast, thyroid, uterine cervix and testis as well as stomach and colon (16).

Both FAM107A (TU3A/DRR1) and FAM107B (HITS) are expected to be tumor suppressors because their expressions are often decreased in cancer cells; moreover, their introduction suppresses cancer cell growth (6,7,10,16,32). HITS possesses a conserved domain of DUF1151 in the N-terminal region, as does FAM107A. However the tissue distribution and the physiological function of HITS are distinctive. First, HITS is expressed in various tissues including digestive, respiratory, genital, and lymphoid organs (Table II and Fig. 1) (16). In contrast, FAM107A is expressed predominantly in the nervous system, especially in neurons, but not in astrocytes or in oligodendrocytes (13,14). Regarding subcellular localization, both HITS and FAM107A are localized in the cell nucleus because of a nuclear localization signal in the center of the protein sequences (16). Second, the HITS gene carries the promoter region providing heat-shock transcription factor 1 (HSF1) binding sites and the transcription of HITS is amplified by heat-shock or hyperthermia treatment (16). This is a salient distinguishing feature of HITS because other HSPs and HSF1 are regarded as having oncogenic activities in many respects (22-24,33-37). In our studies, similarly to FAM107A, ectopic or forced expression of HITS in cancer cells inhibited tumor growth *in vitro* and *in vivo* (Fig. 5) (16). Consequently, HITS is a potential tumor suppressor protein with a unique feature of its transcriptional induction by heat-shock stimulation. It is expected to be useful for tumor diagnosis and for monitoring therapeutic effects of hyperthermia.

A previous study by the authors found that the level of HITS expression in gastrointestinal cancer cells was lower

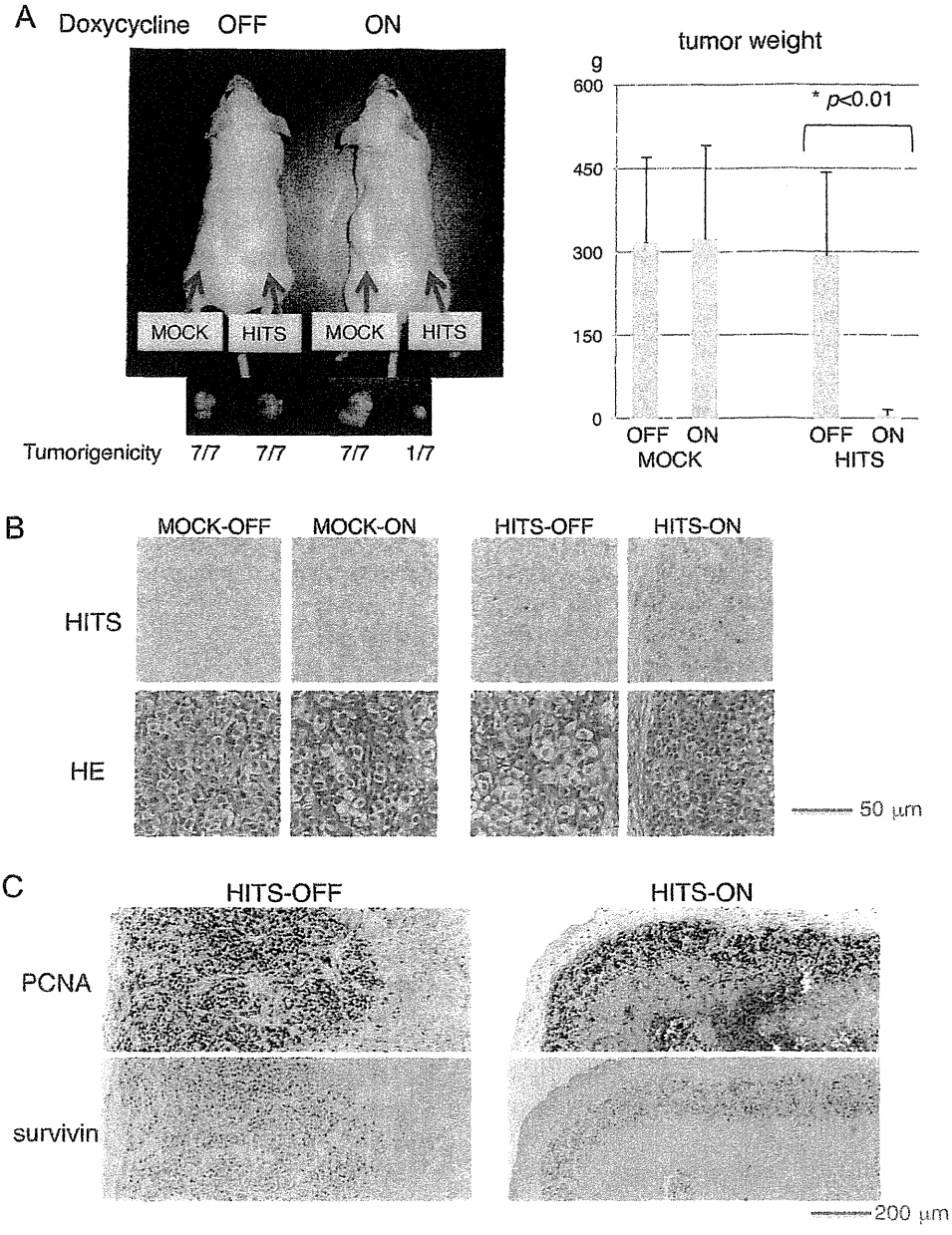

Figure 5. Effects of forced expression of HITS in the uterine cervical cancer xenograft model. (A) *In vivo* tumorigenicity was assayed by inoculating $1x10^6$ HeLa cells transduced with mock or Tet-inducible HITS in Scid mice, with (mouse on the right) or without (mouse on the left) doxycycline administration. Their tumorigenicity was examined at 8 weeks after the respective treatments and is expressed as averages of xenograft weight ± SD (graph). Significance of the difference was determined using two-sided Mann-Whitney U tests. (B and C) Tumors removed from mice were fixed and processed for histopathological and immunohistochemical examinations. (B) HE staining (lower panels) and immunohistochemical staining of HITS (upper panels). (C) Immunohistochemical staining of survivin (lower panels) and PCNA (upper panels). *Denotes a statistically significant effect ($p<0.05$, bracket).

than in normal epithelial cells, although its expression pattern and intensity varied among cancers of different histological types (16). Expression of HITS was decreased during the process of colorectal adenoma-to-carcinoma sequence, and also decreased in intestinal-type gastric adenocarcinomas, but not in diffuse type adenocarcinomas. HITS expression was positive in both stomach and colon mucinous adenocarcinomas. In the present study, tissue microarray analysis revealed that loss of HITS expression in cancer was commonly observed in several organs in a histopathological-type-specific manner. HITS expression was decreased in the prevalent histologic types of breast cancer, invasive ductal, and lobular carcinomas compared with normal breast ducts (Fig. 2A). Statistical analysis elucidated that HITS expression became lower in accordance with breast cancer progression on TNM staging (Table III). It is particularly interesting that, among the factors determining TNM stages, HITS expression scores were inversely correlated with the T-value but not with the N-value. Inverse association with the T-value was also found in thyroid cancer (Fig. 3D).

HITS expression was significantly higher in cancers with a desmoplastic stromal reaction (Fig. 2B and C), similar to diffuse-type gastric cancers with scirrhous stromal reaction that exhibited much higher HITS expression than intestinal-type cancers (16). In further statistical analysis with other pathological parameters of breast cancer, the score of HITS expression correlates positively with expression of HER2 and

Ki-67, and inversely with PR expression (Table III and Fig. 2E). These molecular markers play important roles in carcinogenesis and tumor progression in breast cancers (38-40). Expression levels of HER2, ER and PR are well-established markers for predicting anti-tumor effects of trastuzumab (Herceptin), a therapeutic monoclonal antibody to HER2 and of endocrine therapy, respectively (41,42). Scores of HITS expression are apparently high in HER2 positive, Ki-67 positive, PR negative, and desmoplastic reaction-positive breast cancer, which was thought to be an aggressive phenotype presenting increased risk of disease recurrence and shortened survival (43,44).

Invasive ductal carcinoma of the breast is classified histologically into two subtypes: pure invasive ductal carcinoma (IDC) and IDC associated with ductal carcinoma *in situ* (IDC/DCIS) (40). Pure IDC is morphologically, pathologically, and genetically distinct and has a worse prognosis than IDC/DCIS, suggesting that they might be different biological and clinical tumor entities (33,45-47). HER2 amplification and Ki-67 expression were significantly higher in pure IDC cases than in IDC/DCIS, although the PR expression in pure IDC was significantly lower than in IDC/DCIS. The ER expression and p53 expression showed no statistically significant differences between the two histological subtypes (40). The correlation of HITS expression with the molecular characteristics as described above suggests that the distinct staining pattern of HITS can surrogate the reported difference in molecular characteristics between pure IDC and IDC/DCIS, thereby enabling differential diagnosis of these tumor subtypes with different clinical outcomes.

Considering our results that HITS expression was lost during the course of tumor progression in T-value of TNM grading (Table III and Fig. 3D), it is speculated on one hand that HITS expression decreases during the long process from pre-neoplastic or earlier neoplastic lesions such as DCIS in breast, intestinal metaplasia in stomach, tubular adenoma in colon and CIN in uterine cervix to invasive cancers. On the other hand, HITS expression is preserved in aggressive types of cancers, such as scirrhous-type gastric and breast cancers, which are characterized by distinct genetic alterations and rapid growth or invasions (48,49). Because forced expression of HITS inhibited cancer cell proliferation in response to growth factors and tumor xenograft growth (Fig. 5) (16), we assume that HITS expression influences the primary tumor growth *per se* during tumor development, but that it does not influence the invasion or metastasis, e.g., tumor spread such as scirrhous-type or lymph-node metastasis.

A clear boundary of HITS expression levels was apparent between cancer and non-cancerous lesions e.g. inflammation, benign tumor, and precancerous lesions in thyroid, cervical uterine and testicular tissues (Figs. 3 and 4). Diagnosis of malignancy in thyroid tumors is a difficult task performed using a combination of pathologic examination, blood tests including those of thyroid hormones, and image diagnostic methods such as computed tomography, ultrasound sonography, and scintigraphy. Fine needle aspiration cytology (FNAC) is a useful method to differentiate benign and malignant nodules. However, the sensitivity and specificity of FNAC has been reported, respectively, as 65-98% and 73-100% (50). Our statistical analysis revealed that HITS expression levels in both papillary and follicular types of thyroid carcinoma were significantly lower than in non-cancerous lesions such as adenoma, goiter, and thyroiditis (Fig. 3), suggesting the possibility of using immunohistochemical examination of HITS expression to complement the routine pathology diagnosis of thyroid cancer.

Persistent HPV infection is the primary cause of CIN and invasive cervical cancer. CIN encompasses a continuum of morphologic changes arising in the basal layer of the stratified squamous epithelium of the transformation zone. The mean age of women with CIN is about 15 years younger than the age of those with invasive cancer, suggesting a slow progression of CIN to invasive carcinoma (31). Our result that the HITS expression level was significantly different between CIN and invasive cervical cancer (Fig. 4) indicates that the HITS expression was lost during a course of CIN progression to invasive carcinoma following HPV infection.

The molecular mechanism underlying the biological functions of FAM107 remains unclear. The C-terminal variable regions of FAM107 with a coiled-coil domain are expected to be involved in regulating gene transcription. Recently, it was reported that a point mutation in the C-terminal region of HITS (chromosome10:14603968 C•G→T•A transition) is frequently observed in the primary tumor, brain metastasis and especially in xenograft in genomic analyses of basal-like breast cancer (51). The protein sequence of the C-terminal region is unique to HITS, suggesting its role in tumorigenicity through the transcriptional regulation of oncogenes and tumor-suppressor genes. In contrast, C-terminal coiled-coil domain of FAM107A was reported to associate with and organize the actin and microtubular cytoskeletons and that these associations are essential for focal adhesion (FA) disassembly and cell invasion (14). In fact, FAM107A is highly expressed in the invasive component of gliomas and drives invasion as a new cytoskeletal crosslinker that regulates FA dynamics and cell movement. As expected from the difference of C-terminal sequences between HITS and FAM107A, our preliminary experiments showed no association of HITS with the actin cytoskeleton or regulation of FA dynamics either in neural cells or cancer cells (unpublished observation). The function and molecular interaction of the N-terminal conserved domain (DUF1151) of FAM107 remain to be elucidated, but might play an important role in interacting with other proteins to transduce cellular signals and modulate gene transcription in common with FAM107 family proteins as candidate tumor suppressors.

In conclusion, our study clarified HITS as a potential tumor suppressor belonging to HSPs and as a useful marker for pathological diagnosis for use in cases since expression is often lost in carcinomas in various tissues in histopathological-type-specific manner, and involved in suppression of tumor growth.

Acknowledgements

We thank Atsuko Asaka, Kazumi Tanaka and Yumiko Hoshiba for their technical assistance. This study was supported by Grants-in-Aid for Scientific Research from the Japanese Ministry of Education, Culture, Sports, Science and Technology; Collaborative Research (C2011-1) of Kanazawa Medical University.

References

1. Rual JF, Venkatesan K, Hao T, *et al*: Towards a proteome-scale map of the human protein-protein interaction network. Nature 437: 1173-1178, 2005.
2. Ewing RM, Chu P, Elisma F, *et al*: Large-scale mapping of human protein-protein interactions by mass spectrometry. Mol Syst Biol 3: 89, 2007.
3. Stelzl U, Worm U, Lalowski M, *et al*: A human protein-protein interaction network: a resource for annotating the proteome. Cell 122: 957-968, 2005.
4. Wang YL, Faiola F, Xu M, Pan S and Martinez E: Human ATAC Is a GCN5/PCAF-containing acetylase complex with a novel NC2-like histone fold module that interacts with the TATA-binding protein. J Biol Chem 283: 33808-33815, 2008.
5. Frijters R, Fleuren W, Toonen EJ, *et al*: Prednisolone-induced differential gene expression in mouse liver carrying wild type or a dimerization-defective glucocorticoid receptor. BMC Genomics 11: 359, 2010.
6. Yamato T, Orikasa K, Fukushige S, Orikasa S and Horii A: Isolation and characterization of the novel gene, TU3A, in a commonly deleted region on 3p14.3-->p14.2 in renal cell carcinoma. Cytogenet Cell Genet 87: 291-295, 1999.
7. Wang L, Darling J, Zhang JS, *et al*: Loss of expression of the DRR 1 gene at chromosomal segment 3p21.1 in renal cell carcinoma. Genes Chromosomes Cancer 27: 1-10, 2000.
8. van den Boom J, Wolter M, Blaschke B, Knobbe CB and Reifenberger G: Identification of novel genes associated with astrocytoma progression using suppression subtractive hybridization and real-time reverse transcription-polymerase chain reaction. Int J Cancer 119: 2330-2338, 2006.
9. Vanaja DK, Ballman KV, Morlan BW, *et al*: PDLIM4 repression by hypermethylation as a potential biomarker for prostate cancer. Clin Cancer Res 12: 1128-1136, 2006.
10. Liu Q, Zhao XY, Bai RZ, *et al*: Induction of tumor inhibition and apoptosis by a candidate tumor suppressor gene DRR1 on 3p21.1. Oncol Rep 22: 1069-1075, 2009.
11. Kholodnyuk ID, Kozireva S, Kost-Alimova M, Kashuba V, Klein G and Imreh S: Down regulation of 3p genes, LTF, SLC38A3 and DRR1, upon growth of human chromosome 3-mouse fibrosarcoma hybrids in severe combined immunodeficiency mice. Int J Cancer 119: 99-107, 2006.
12. Zhao XY, Liang SF, Yao SH, *et al*: Identification and preliminary function study of *Xenopus laevis* DRR1 gene. Biochem Biophys Res Commun 361: 74-78, 2007.
13. Asano Y, Kishida S, Mu P, Sakamoto K, Murohara T and Kadomatsu K: DRR1 is expressed in the developing nervous system and downregulated during neuroblastoma carcinogenesis. Biochem Biophys Res Commun 394: 829-835, 2010.
14. Le PU, Angers-Loustau A, de Oliveira RMW, *et al*: DRR drives brain cancer invasion by regulating cytoskeletal-focal adhesion dynamics. Oncogene 29: 4636-4647, 2010.
15. Schmidt MV, Schulke JP, Liebl C, *et al*: Tumor suppressor down-regulated in renal cell carcinoma 1 (DRR1) is a stress-induced actin bundling factor that modulates synaptic efficacy and cognition. Proc Natl Acad Sci USA 108: 17213-17218, 2011.
16. Nakajima H, Ishigaki Y, Xia QS, *et al*: Induction of HITS, a newly identified family with sequence similarity 107 protein (FAM107B), in cancer cells by heat shock stimulation. Int J Oncol 37: 583-593, 2010.
17. Jameel A, Skilton RA, Campbell TA, Chander SK, Coombes RC and Luqmani YA: Clinical and biological significance of HSP89 alpha in human breast cancer. Int J Cancer 50: 409-415, 1992.
18. Takayama S, Reed JC and Homma S: Heat-shock proteins as regulators of apoptosis. Oncogene 22: 9041-9047, 2003.
19. Foster CS, Dodson AR, Ambroisine L, *et al*: Hsp-27 expression at diagnosis predicts poor clinical outcome in prostate cancer independent of ETS-gene rearrangement. Br J Cancer 101: 1137-1144, 2009.
20. Ciocca DR, Clark GM, Tandon AK, Fuqua SA, Welch WJ and McGuire WL: Heat shock protein hsp70 in patients with axillary lymph node-negative breast cancer: prognostic implications. J Natl Cancer Inst 85: 570-574, 1993.
21. Nanbu K, Konishi I, Mandai M, *et al*: Prognostic significance of heat shock proteins HSP70 and HSP90 in endometrial carcinomas. Cancer Detect Prev 22: 549-555, 1998.
22. Jolly C and Morimoto RI: Role of the heat shock response and molecular chaperones in oncogenesis and cell death. J Natl Cancer Inst 92: 1564-1572, 2000.
23. Rohde M, Daugaard M, Jensen MH, Helin K, Nylandsted J and Jaattela M: Members of the heat-shock protein 70 family promote cancer cell growth by distinct mechanisms. Genes Dev 19: 570-582, 2005.
24. Whitesell L and Lindquist SL: HSP90 and the chaperoning of cancer. Nat Rev Cancer 5: 761-772, 2005.
25. Mai W, Kawakami K, Shakoori A, *et al*: Deregulated GSK3(beta) sustains gastrointestinal cancer cells survival by modulating human telomerase reverse transcriptase and telomerase. Clin Cancer Res 15: 6810-6819, 2009.
26. Belkacemi Y, Bousquet G, Marsiglia H, *et al*: Phyllodes tumor of the breast. Int J Radiat Oncol Biol Phys 70: 492-500, 2008.
27. Woodward WA, Strom EA, Tucker SL, *et al*: Changes in the 2003 American Joint Committee on Cancer staging for breast cancer dramatically affect stage-specific survival. J Clin Oncol 21: 3244-3248, 2003.
28. Pusztai L, Cristofanilli M and Paik S: New generation of molecular prognostic and predictive tests for breast cancer. Semin Oncol 34: S10-S16, 2007.
29. Kollias J, Elston CW, Ellis IO, Robertson JF and Blamey RW: Early-onset breast cancer - histopathological and prognostic considerations. Br J Cancer 75: 1318-1323, 1997.
30. Bosch FX and de Sanjose S: Chapter 1: Human papillomavirus and cervical cancer - burden and assessment of causality. J Natl Cancer Inst Monogr pp3-13, 2003.
31. Kivlahan C and Ingram E: Papanicolaou smears without endocervical cells. Are they inadequate? Acta Cytol 30: 258-260, 1986.
32. Awakura Y, Nakamura E, Ito N, Kamoto T and Ogawa O: Methylation-associated silencing of TU3A in human cancers. Int J Oncol 33: 893-899, 2008.
33. Park K, Han S, Kim HJ, Kim J and Shin E: HER2 status in pure ductal carcinoma in situ and in the intraductal and invasive components of invasive ductal carcinoma determined by fluorescence in situ hybridization and immunohistochemistry. Histopathology 48: 702-707, 2006.
34. Dai C, Whitesell L, Rogers AB and Lindquist S: Heat shock factor 1 is a powerful multifaceted modifier of carcinogenesis. Cell 130: 1005-1018, 2007.
35. Jego G, Hazoume A, Seigneuric R and Garrido C: Targeting heat shock proteins in cancer. Cancer Lett: Nov 13, 2010 (available online).
36. Wang RE: Targeting heat shock proteins 70/90 and proteasome for cancer therapy. Curr Med Chem 18: 4250-4264, 2011.
37. Khalil AA, Kabapy NF, Deraz SF and Smith C: Heat shock proteins in oncology: diagnostic biomarkers or therapeutic targets? Biochim Biophys Acta 1816: 89-104, 2011.
38. Dalton LW, Page DL and Dupont WD: Histologic grading of breast carcinoma. A reproducibility study. Cancer 73: 2765-2770, 1994.
39. Tsuda H, Akiyama F, Kurosumi M, Sakamoto G and Watanabe T: Establishment of histological criteria for high-risk node-negative breast carcinoma for a multi-institutional randomized clinical trial of adjuvant therapy. Japan National Surgical Adjuvant Study of Breast Cancer (NSAS-BC) Pathology Section. Jpn J Clin Oncol 28: 486-491, 1998.
40. Mylonas I, Makovitzky J, Jeschke U, Briese V, Friese K and Gerber B: Expression of Her2/neu, steroid receptors (ER and PR), Ki67 and p53 in invasive mammary ductal carcinoma associated with ductal carcinoma in situ (DCIS) versus invasive breast cancer alone. Anticancer Res 25: 1719-1723, 2005.
41. Lower EE, Glass EL, Bradley DA, Blau R and Heffelfinger S: Impact of metastatic estrogen receptor and progesterone receptor status on survival. Breast Cancer Res Treat 90: 65-70, 2005.
42. Wolff AC, Hammond ME, Schwartz JN, *et al*: American Society of Clinical Oncology/College of American Pathologists guideline recommendations for human epidermal growth factor receptor 2 testing in breast cancer. J Clin Oncol 25: 118-145, 2007.
43. Narod SA, Brunet JS, Ghadirian P, *et al*: Tamoxifen and risk of contralateral breast cancer in BRCA1 and BRCA2 mutation carriers: a case-control study. Hereditary Breast Cancer Clinical Study Group. Lancet 356: 1876-1881, 2000.
44. Schnitt SJ: Estrogen receptor testing of breast cancer in current clinical practice: what's the question? J Clin Oncol 24: 1797-1799, 2006.
45. Farabegoli F, Champeme MH, Bieche I, *et al*: Genetic pathways in the evolution of breast ductal carcinoma in situ. J Pathol 196: 280-286, 2002.
46. Jo BH and Chun YK: Heterogeneity of invasive ductal carcinoma: proposal for a hypothetical classification. J Korean Med Sci 21: 460-468, 2006.

47. Steinman S, Wang J, Bourne P, Yang Q and Tang P: Expression of cytokeratin markers, ER-alpha, PR, HER-2/neu, and EGFR in pure ductal carcinoma in situ (DCIS) and DCIS with co-existing invasive ductal carcinoma (IDC) of the breast. Ann Clin Lab Sci 37: 127-134, 2007.
48. Lauren PA and Nevalainen TJ: Epidemiology of intestinal and diffuse types of gastric carcinoma. A time-trend study in Finland with comparison between studies from high- and low-risk areas. Cancer 71: 2926-2933, 1993.
49. Walker RA: The complexities of breast cancer desmoplasia. Breast Cancer Res 3: 143-145, 2001.
50. Haberal AN, Toru S, Ozen O, Arat Z and Bilezikci B: Diagnostic pitfalls in the evaluation of fine needle aspiration cytology of the thyroid: correlation with histopathology in 260 cases. Cytopathology 20: 103-108, 2009.
51. Ding L, Ellis MJ, Li S, *et al*: Genome remodelling in a basal-like breast cancer metastasis and xenograft. Nature 464: 999-1005, 2010.

Yoshimi et al. BMC Cancer 2012, 12:448
http://www.biomedcentral.com/1471-2407/12/448

BMC Cancer

RESEARCH ARTICLE Open Access

Use of a chemically induced-colon carcinogenesis-prone *Apc*-mutant rat in a chemotherapeutic bioassay

Kazuto Yoshimi[1], Takao Hashimoto[2], Yusuke Niwa[2], Kazuya Hata[2], Tadao Serikawa[1], Takuji Tanaka[3] and Takashi Kuramoto[1*]

Abstract

Background: Chemotherapeutic bioassay for colorectal cancer (CRC) with a rat model bearing chemically-induced CRCs plays an important role in the development of new anti-tumor drugs and regimens. Although several protocols to induce CRCs have been developed, the incidence and number of CRCs are not much enough for the efficient bioassay. Recently, we established the very efficient system to induce CRCs with a chemically induced-colon carcinogenesis-prone *Apc*-mutant rat, Kyoto Apc Delta (KAD) rat. Here, we applied the KAD rat to the chemotherapeutic bioassay for CRC and showed the utility of the KAD rat.

Methods: The KAD rat has been developed by the ENU mutagenesis and carries a homozygous nonsense mutation in the *Apc* gene (S2523X). Male KAD rats were given a single subcutaneous injection of AOM (20 mg/kg body weight) at 5 weeks of age. Starting at 1 week after the AOM injection, they were given 2% DSS in drinking water for 7 days. Tumor-bearing KAD rats were divided into experimental and control groups on the basis of the number of tumors observed by endoscopy at week 8. The 5-fluorouracil (5-FU) was administrated intravenously a dose of 50 or 75 mg/kg weekly at week 9, 10, and 11. After one-week interval, the 5-FU was given again at week 13, 14, and 15. At week 16, animals were sacrificed and tumor number and volume were measured macroscopically and microscopically.

Results: In total 48 tumors were observed in 27 KAD rats with a 100% incidence at week 8. The maximum tolerated dose for the KAD rat was 50 mg/kg of 5-FU. Macroscopically, the number or volume of tumors in the 5-FU treated rats was not significantly different from the control. Microscopically, the number of adenocarcinoma in the 5-FU treated rats was not significantly different ($p < 0.02$) from that of the control. However, the volume of adenocarcinomas was significantly lower than in the control. Anticancer effect of the 5-FU could be obtained only after the 16 weeks of experimental period.

Conclusion: The use of the AOM/DSS-treated tumor-bearing KAD rats could shorten the experimental period and reduce the number of animals examined in the chemotherapeutic bioassay. The efficient bioassay with the AOM/DSS-treated tumor-bearing KAD rats would promote the development of new anti-tumor drugs and regimens.

Keywords: Adenomatous polyposis coli, Colorectal cancer, Endoscopy, Rat, Chemotherapy, 5-fluorouracil

* Correspondence: tkuramot@anim.med.kyoto-u.ac.jp
[1]Institute of Laboratory Animals, Graduate School of Medicine, Kyoto University, Yoshidakonoe-cho, Sakyo-ku, Kyoto 606-8501, Japan
Full list of author information is available at the end of the article

Background

Chemotherapeutic bioassays for colorectal cancer (CRC) play an important role in the development of new anti-tumor drugs and regimens. These bioassays involve the use of colon carcinogenesis models which mainly consist of animal xenografts, an adenomatous polyposis coli (*Apc*)-mutant mouse model and a chemically-induced CRC model [1-3].

The xenograft model utilizes cultured or primary CRC cells that are implanted under the skin of immune-deficient mice and rats. The size and volume of tumors can be estimated easily and temporally by measuring their dimensions. However, these animals have defects in the immune system that suppresses tumor growth. The subcutaneous microenvironment around the transplanted tumors differs from the colon environment in which the original CRC of the cell lines arose. Therefore, this approach appears to ignore the contribution of the tumor microenvironment and does not exactly mimic tumor development in man [4,5].

Apc-mutant mouse models, such as the Min mouse model, spontaneously develop a considerable number of intestinal tumors and have been widely used as a relevant model for evaluating human chemopreventative therapies. However, tumors in the colon are developed at a much lower frequency than in the small intestine. Even if tumors do develop in the colon, almost all of them are low grade adenomas [6].

The chemically-induced CRC model is superior to these models in that the characteristics of the induced tumor are very similar to those of human CRC. Tumors only develop in the colon through multi-step carcinogenesis which mimics the entire process of tumor growth in man. In this model, tumor morphology and mutation spectrum are also similar to those in human CRC [6]. Moreover, methods of inducing colon tumors are well-established, so that we can be certain of obtaining the number of tumors expected, which is ideal for the evaluation of potential chemotherapeutic drugs [2,7].

Although many carcinogens induce colon tumors in rats, azoxymethane (AOM) administered subcutaneously has been most widely used [2,6,8]. However, the incidence of colon tumors induced by two or three subcutaneous injections of AOM is not high, and it takes 7–9 months to induce sufficient tumors to evaluate the chemotherapeutic efficacy of potential anti-cancer drugs [9]. Such limitations have been significantly improved by using dextran sodium sulfate (DSS) as an inflammatory agent. When 2% DSS is administered in drinking water to the AOM-treated rats for one week, starting one week after administration, a number of colon tumors develop within a short time period (this is known as the TANAKA method) [10].

Recently we developed a novel *Apc* mutant rat strain, called the Kyoto Apc Delta (KAD) rat (strain name: F344-*Apc*^{m1kyo}) from our ENU-mutagenesis program. The KAD rat carries a homozygous nonsense mutation in the *Apc* gene (S2523X). Thus, the KAD rat lacks 321-amino acids in the C-terminal of APC, but it remains viable at almost 2 years and shows no spontaneous colorectal tumors. Moreover, by applying the TANAKA method to KAD rats, we obtained a much higher incidence, multiplicity and malignancy of colon tumors in KAD rats than colon tumors in F344 wild rats. We were able to induce these tumors within 15 weeks of the experimental period. In addition, we were able to carry out endoscopic observation, by which colon tumors could be detected from Week 8 [11].

In the present study, in order to establish an efficient chemotherapeutic bioassay with KAD rats, we induced colon tumors by means of treatment with AOM and DSS, and then administered a typical anti-tumor drug, namely 5-fluorouracil (5-FU) to the tumor-bearing rats.

Methods

Chemicals

5-FU was purchased from Kyowa Hakko Kogyo, Co., Ltd. (Tokyo, Japan). AOM was purchased from Sigma-Aldrich Chemical Co. (St. Louis, MO, USA). These drugs were diluted in saline just before administration. DSS (MW 36,000–50,000) was purchased from ICN Biochemicals, Inc. (Aurora, OH, USA). DSS was dissolved in distilled water at 2% (w/v) every day before treatment.

Rats

Specific pathogen free male KAD rats were purchased from Japan SLC, Inc. (Hamamatsu, Japan) and provided by the National Bio Resource Project for the Rat (http://www.anim.med.kyoto-u.ac.jp/nbr) at 4 weeks of age. The rats were acclimatized for a week before the experiment and were maintained under conditions of 50 ± 10% humidity, 12 h-12 h light cycle and 24 ± 2 °C temperature. They were fed a standard pellet diet (F-2, Funabashi Farm, Funabashi, Japan) and tap water *ad libitum*.

Induction of colon tumor

Chemically induced-colon carcinogenesis was carried out as described in our previous study [11]. Briefly, male KAD rats (n = 32) were given a single subcutaneous injection of AOM (20 mg/kg body weight) at 5 weeks of age. Starting at 1 week after the AOM injection, they were given 2% DSS in drinking water for 7 days (Figure 1). Five rats were used to find correlation of the number of polypoid lesions with the volume of tumors at Week 8. All experimental procedures were approved by the Animal Research Committee of Kyoto University

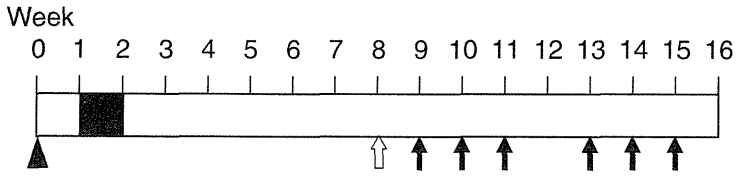

Figure 1 Experimental schedule. KAD rats at 5 weeks of age were given a subcutaneous injection of AOM at 20 mg/kg body weight (arrow head). One week after the AOM injection they were given 2% DSS (MW 36,000–50,000) in their drinking water for one week (black box). Endoscopic observation was carried out at week 8 (open arrow). 5-FU was administrated intravenously at weeks 9, 10, 11, 13, 14 and 15 (arrows). All animals were sacrificed at week 16.

and were performed according to the Regulation on Animal Experimentation at Kyoto University.

Endoscopic observation

Observation was performed at week 8 with an endoscope (BF TYPE 3C40: Olympus, Tokyo, Japan) to determine the presence of colon tumors (Figure 1). KAD rats were anesthetized by administration of 2% isoflurane (Forane: Abbott Japan, Tokyo, Japan) vapor through a nose cone. The colon was flushed using an enema of tap water to remove feces. The endoscope was inserted into the colon, and endoscopic images were acquired within the distal colon and rectum. The numbers of polypoid lesions, assumed to be developing colorectal tumors, were counted.

Chemotherapeutic test

The AOM/DSS-treated rats were divided into three groups (nine rats each), among which numbers of colon tumors were not significantly different. The 5-FU was administrated to the tumor-bearing KAD rats at two different doses (50 or 75 mg/kg) by three weekly intravenous (i.v.) injections at weeks 9, 10 and 11. According to the preliminary experiment, we set a 1 week withdrawal period to decrease the occurrence of serious side effects caused by 5-FU. One week later, rats underwent additional administration of 5-FU involving three weekly i.v. injections at weeks 13, 14 and 15. At week 16 animals were sacrificed by cervical dislocation under anesthesia with isoflurane (Figure 1). Then the colorectum of the rats was resected, washed with PBS, opened longitudinally along the main axis and fixed in 10% neutral buffered formalin for at least 24 h. The number and volume of colon tumors were measured after fixation. The other organs such as small intestine, stomach, liver and kidney were observed macroscopically for any abnormalities.

Histopathological examination

After careful macroscopic inspection, tumors and whole colonic mucosa were embedded in paraffin and sectioned for histopathology after staining with hematoxylin and eosin. After tumors that developed in the colorectum were photographed, the largest and the smallest superficial diameters of adenocarcinoma that were diagnosed histopathologically were measured on the photographs. Tumor volume was calculated according to the formula $V = a \times b^2/2$, in which "a" is the largest superficial diameter and "b" is the smallest superficial diameter [12].

Immunohistochemistry

Cell proliferation and apoptosis were evaluated by determination of the percentages of PCNA- and cleaved caspase-3-positive nuclei in a total of 200 cancer cells for each sample ($n = 6$ from the control group and $n = 8$ from Group 1). Briefly, sections were incubated with anti-mouse PCNA antibody (clone PC10, 1:1000 dilution; DAKO) and cleaved caspase-3 (Asp175) antibody (1:1000 dilution; Cell Signaling Technology) overnight at 4 °C. Biotinyl antibody was used as secondary antibody and then the streptavidin-peroxidase complex (LASB^{TM} + Kit, Universal, DAKO) was applied. The antigen-antibody complex was visualized by 3,3′-diamonobenzidine tetrachloride (DAKO).

Statistical analysis

Data are expressed as the mean ± standard deviation (S.D.). Student's *t*-test was performed using the statistics package within Microsoft Excel for statistical analysis, and p values were considered significant when < 0.05.

Results

Correlation of the number of polypoid lesions with the total volume of tumors

To find the correlation of the number of polypoid lesions with the total volume of tumors, we induced colon tumors to KAD rats ($n = 5$) by the TANAKA method and counted tumor number under the endoscopy and the number and volume of tumors under the microscopy at week 8 (Additional file 1: Table S1). As a good correlation between them was found, it is very likely that the number of polypoid lesions found with the endoscopy at week 8 can be used to estimate the total volume of tumors (Additional file 2: Figure S1).

Effective tumor development in AOM/DSS-treated KAD rats

At week 8 when carrying out endoscopic observations for the occurrence of colon tumors in the colons of AOM/DSS-treated KAD rats, we could observe about 10 cm of the luminal surface, from the rectum to the distal colon. We found polypoid lesions around the rectum and the distal colon. Polypoid lesions which were clearly different from normal mucosa assumed to be developing colorectal tumors. All AOM/DSS-treated KAD rats developed colon tumors. In total 48 tumors were observed in 27 KAD rats with a 100% incidence and a multiplicity of 1.78 ± 0.85, ranging from 1 to 4 per rat.

Dosing condition of 5-FU

On the basis of the number of tumors, the tumor-bearing KAD rats were divided into three groups. One was the control group and the others were experimental groups, in which rats were given 5-FU at a concentration of 50 mg/kg (Group 1) or 75 mg/kg (Group 2). Each group consisted of nine rats and the total number of tumors in each group was 16. The average number of tumors per rat was not significantly different among the groups (Control: 1.78 ± 0.83, Group 1: 1.78 ± 0.83, Group 2: 1.78 ± 0.97) (Figure 2B).

The average body weight of rats in Group 1 tended to be lower than in the control group, and was significantly different from the control group at weeks 15 (300.0 ± 18.1 vs 319.4 ± 20.1; $p < 0.05$) and 16 (296.1 ± 18.9 vs 318.8 ± 18.8; $p < 0.03$). However the reduction in body weight was less than 10% as compared with the control. None of the rats in Group 1 died during the experiment. On the other hand, gain in body weight in Group 2 was constantly and significantly impaired throughout the experimental period. More than 10% of weight loss was observed at weeks 12, 15 and 16, as compared with that in the control group (Figure 3A). KAD rats in Group 2 had severe bloody stools and diarrhea and six rats (67%) in the group died during the experiment (Figure 3B). These findings indicated that the 75 mg/kg dose of 5-FU was too toxic for the tumor-bearing KAD rats, and led to the marked body weight loss and eventually to death. Thus, the 50 mg/kg dose of 5-FU was considered to be appropriate for evaluation of the antitumor activity of 5-FU, when we used the tumor-bearing KAD rats in a chemotherapeutic bioassay.

Reduction of volume but not number of adenocarcinomas in the tumor-bearing KAD rats by treatment with 5-FU

At week 16 we carried out an autopsy and macroscopic examination of the large bowels of the control group and Group 1. Macroscopically, rats in both groups developed multiple nodular, polypoid or caterpillar-like tumors mainly in the rectum and distal colon (Figure 4). The number of tumors in Group 1 was not significantly different from the control group (Table 1). The volume of tumors, which were macroscopically calculated, was 27% smaller in Group 1 than in the control group, but the difference was not significant ($p = 0.34$).

Microscopically, all tumors that developed in KAD rats were tubular adenoma or well- or moderately-differentiated tubular adenocarcinoma (Figure 5A and 5B). The multiplicity of adenoma or adenocarcinoma in Group 1 was not significantly different from that of the control group ($p = 0.53$; $p = 0.44$, respectively) (Table 1). The size of the adenomas was too small for their volumes to be calculated. However, the volume of adenocarcinomas (63.85 ± 51.06 mm^3) in Group 1 was significantly lower ($p < 0.02$) than in the control group (34.40 ± 31.26 mm^3), when the volume was calculated from the histological sections. In addition, we found significant reduction of PCNA labeling index as well as

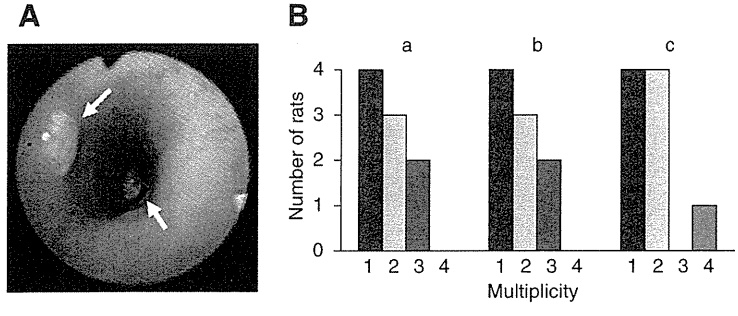

Figure 2 Grouping of AOM/DSS-treated KAD rats before 5-FU treatment. (**A**) Endoscopic view of colon tumors (arrows) in an AOM/DSS-treated KAD rat at week 8. (**B**) AOM/DSS-treated KAD rats were divided into experimental groups based on the number of tumors induced in their colons. The number of tumors induced in each animal determined by endoscopic observations varied from one to four. In total, 48 tumors were found in 27 rats. The tumor-bearing rats (nine per group) were divided into three groups (a: saline, b: 50 mg/kg 5-FU and c: 75 mg/kg 5-FU), so as not to be significantly different at the starting point of treatments.

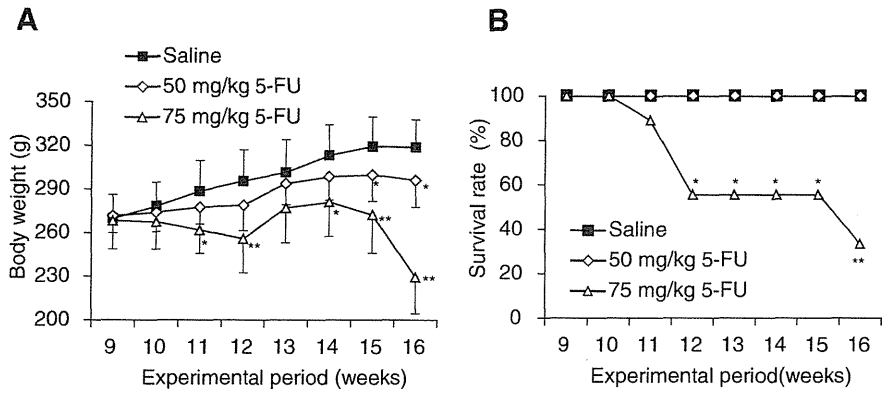

Figure 3 Toxicity of 5-FU in AOM/DSS treated KAD rats. Average body weight (**A**) and survival rate (**B**) of the control, 50 mg/kg and 75 mg/kg 5-FU treated groups. *$p < 0.05$, **$p < 0.001$.

significant elevation of cleaved caspase-3 positive rate in the adenocarcinomas in Group 1 (Figure 6). These results suggest that the 5-FU treatment suppressed cell proliferation and induced apoptosis and thereby inhibited adenocarcinoma development.

Discussion

Carcinogenic process is complex. Tumor development proceeds via a multi-step process, in which a succession of genetic changes, each conferring one or another type of growth advantage, leads to the progressive conversion of normal cells into cancer cells. Moreover, extent of cell transformation depends on the genetic predisposition and environmental factors [13]. Thus, to obtain cancerous lesions effectively, it is necessary to use a synergy effect of genetic and environmental factors. Our carcinogenic system with KAD rats employs such synergy effect of *Apc*-mutation, chemical carcinogen exposure, and tissue inflammation.

In ideal chemotherapeutic bioassay systems, the number and volume of tumors should be evaluated as the indicator of anti-tumor drug efficacy. Therefore, it is indispensable to be able to strictly set the size of the experimental and control groups, among which the number and volume of tumors should not differ significantly. To this end, we carried out endoscopic observations in the colons of AOM/DSS-treated KAD rats, and divided animals into groups on the basis of the number of colon tumors. Since the rat has a suitable body size for handling, we could easily manipulate the endoscope and correctly count the number of tumors. At week 8 we found colon tumors with a 100% incidence in AOM/DSS-treated KAD rats. The rats developed one to four tumors. On the basis of the number of tumors, we could set the experimental and control groups, because

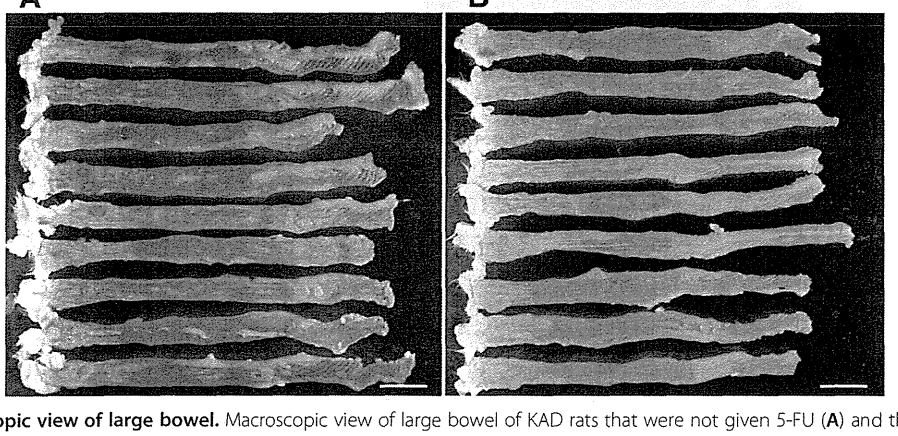

Figure 4 Macroscopic view of large bowel. Macroscopic view of large bowel of KAD rats that were not given 5-FU (**A**) and that were given 50 mg/kg 5-FU (**B**). Colon tumors that developed in both groups were mainly distributed in the rectum and distal colon, which was assumed to be within 8 cm from the anus. No tumors were observed in the proximal colon. Left side: anus. Right side: cecum. Bar: 2 cm.

Table 1 Effects of 5-FU on the development of colon tumors in the KAD rat

Treatment	No. of rats	Macroscopic observation		Microscopic observation			
		Multiplicity	Volume (mm^3)[1]	Multiplicity			Volume (mm^3)[2]
				adenomas	adenocarcinomas	total	adenocarcinoma
Saline	9	5.56 ± 3.43	106.34 ± 68.92	3.11 ± 2.52	3.22 ± 2.77	6.33 ± 4.87	63.85 ± 51.06
50 mg/kg 5-FU	9	6.33 ± 3.04	77.28 ± 57.23	3.78 ± 1.79	2.33 ± 1.94	6.11 ± 2.37	34.40 ± 31.26 [3]

[1]Tumor volume was determined by the formula $V = a \times b^2/2$ (V: volume. a: the largest superficial diameter and b: the smallest superficial diameter).
[2]Volumes of adenomas were too small to calculate.
[3]Adenocarcinoma volumes observed in the 5-FU-treated KAD rats were significantly reduced as compared with those of non-treated rats ($p < 0.02$).

the number of tumors observed by the endoscopy is correlated to the volume of tumors obtained by the microscopy at week 8. We, therefore, recommend counting the number of tumors using endoscopic observation before dividing the rats into groups.

It is important to identify biomarkers that are used to predict efficacy and safety of anti-tumor drugs. Rats can be subjected to the sequential sampling of bloods. The amounts of bloods or urines are enough to be examined. Moreover, drug kinetics can be monitored by *in vivo* imaging [14]. Thus, the chemotherapeutic bioassay with the KAD rats is a candidate system to explore the biomarkers.

5-FU is a pyrimidine analog and when incorporated into DNA inhibits the cell's ability to synthesize DNA. Eventually 5-FU induces cell cycle arrest and apoptosis, mainly in cells with high proliferative activity such as cancer cells [15]. Side effects of 5-FU, such as diarrhea and weight loss, are problematic in performing chemotherapeutic tests with animal models. Thus, it is important to determine the maximum tolerated dose (MTD) that does not produce profound weight loss, and that causes no drug-related lethality. Usually the MTD of 5-FU in rats ranges from 25 to 100 mg/kg, depending on the 5-FU administration schedules [16]. In the current study, we found that the MTD was 50 mg/kg of 5-FU when administered to tumor-bearing KAD rats by i.v. injection. Although the MTD should be determined using different administration schedules and routes, the MTD that we determined in the present study can be a helpful guide in setting doses of anti-cancer drugs in further chemotherapeutic tests with KAD rats.

In our study, the treatment of tumor-bearing KAD rats with 5-FU failed to reduce the multiplicity of adenoma or adenocarcinoma. However, the treatment significantly reduced adenocarcinoma tumor volume and cell proliferation as well as increased adenocarcinoma apoptosis, which was consistent with the mode of action of the 5-FU [15]. Treatment response assessed in terms of

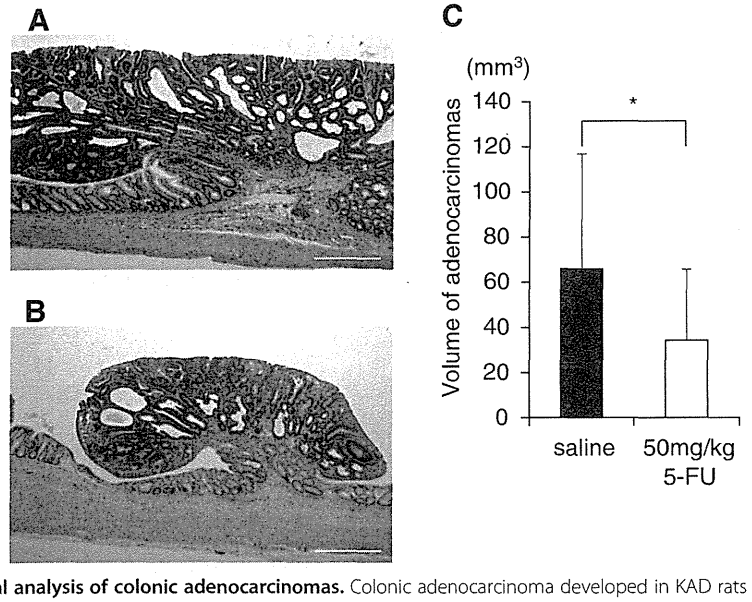

Figure 5 Histopathological analysis of colonic adenocarcinomas. Colonic adenocarcinoma developed in KAD rats that were not given 5-FU (**A**) and that were given 50 mg/kg 5-FU (**B**). Most of the adenocarcinomas in KAD rats that received 50 mg/kg 5-FU were smaller than those in the control group (hematoxylin and eosin stain). Bar: 500 μm. (**C**) Average volume of adenocarcinoma tumors grown in KAD rats that were given saline or 5-FU (50 mg/kg). The mean volume of adenocarcinoma tumors in the 5-FU-treated rats were significantly smaller than those in the non-treated rats. *: $p < 0.02$.

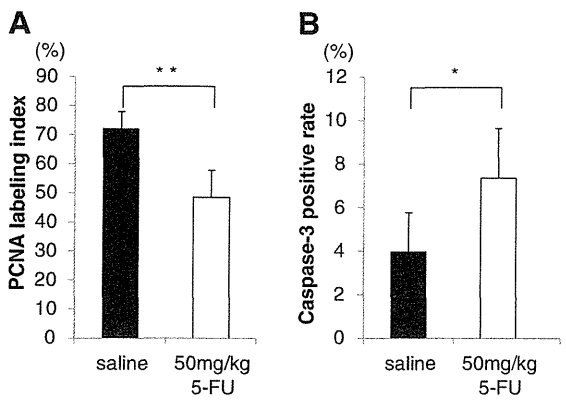

Figure 6 Cell proliferation and apoptosis in adenocarcinomas of the 5-FU treated KAD rats. (**A**) The PCNA labeling index was significantly lower in the 5-FU treated KAD rats (50 mg/kg) than that in the control KAD rats, indicating significant decrease in cell proliferation in the adenocarcinomas. **: $p < 0.001$. (**B**) The cleaved caspase-3 positive rate was significantly higher in the 5-FU treated KAD rats (50 mg/kg) than that in the control KAD rats, indicating significant increase in apoptosis in the adenocarcinomas. *: $p < 0.02$.

change in tumor size after 5-FU administration in the present study amounted to a 30% reduction, which was similar to the response rate of 5-FU as a single agent seen in human cancers, including CRC [17]. These findings indicated that the response of tumors in AOM/DSS-treated KAD rats to 5-FU treatment was similar to human CRC, and supported the view that this should be a useful bioassay system for employment in further chemotherapeutic studies.

Conclusions

In the present study we established a chemotherapeutic bioassay system for CRC using KAD rats. In this system, we could set the experimental groups on the basis of the number of tumors detected by endoscopic examination. After 5-FU administration rat colon tumors induced by AOM/DSS treatments showed a similar response, in terms of percentage reduction in size and cell proliferation and percentage elevation in apoptosis, to those reported in clinical CRC studies. Thus, we expect that this system could effectively promote the development of new anti-tumor drugs and regimens for human CRC.

Additional files

Additional file 1: Table S1. Number and total volume of tumors found in KAD rats at week 8.

Additional file 2: Figure S1. The correlation of total volume of tumors with the numbers of polypoid lesions observed by endoscopy at Week8. Regression formula was made with Excel software package (Microsoft). Vertical axis was shown in logarithmic scale.

Competing interests

The authors declare that they have no competing interests.

Authors' contributions

KY and TK conceived the study and designed the experiments. KY, TH, YN and KH performed the experiments. TT performed the histopathological analysis. KY, TK and TT wrote the manuscript. TS revised the manuscript. All authors have read and approved the final manuscript.

Acknowledgments

This work was supported in part by a Grant-in-Aid for Cancer Research from the Ministry of Health, Labour and Welfare (to TK), and Grants-in-Aid for Scientific Research from the Japan Society for the Promotion of Science (21300153 to TK and 0233639 to KY). The KAD (F344-*Apc*^{m1Kyo}) rat has been deposited in the National BioResource Project-Rat in Japan and is available from the Project (http://www.anim.med.kyoto-u.ac.jp/nbr).

Author details

[1]Institute of Laboratory Animals, Graduate School of Medicine, Kyoto University, Yoshidakonoe-cho, Sakyo-ku, Kyoto 606-8501, Japan. [2]Sunplanet Co., Ltd, 4388 Makita, Kamiishizu, Ogaki 503-1602, Japan. [3]Cancer Research and Prevention, The Tohkai Cytopathology Institute, 4-33 Minami-Uzura, Gifu 500-8285, Japan.

Received: 24 April 2012 Accepted: 26 September 2012
Published: 3 October 2012

References

1. Blumenthal RD, Osorio L, Hayes MK, Horak ID, Hansen HJ, Goldenberg DM: Carcinoembryonic antigen antibody inhibits lung metastasis and augments chemotherapy in a human colonic carcinoma xenograft. *Cancer Immunol Immunother* 2005, 54(4):315–327.
2. Corpet DE, Pierre F: Point: From animal models to prevention of colon cancer. Systematic review of chemoprevention in min mice and choice of the model system. *Cancer Epidemiol Biomarkers Prev* 2003, 12(5):391–400.
3. Williams KJ, Telfer BA, Stratford IJ, Wedge SR: ZD1839 ('Iressa'), a specific oral epidermal growth factor receptor-tyrosine kinase inhibitor, potentiates radiotherapy in a human colorectal cancer xenograft model. *Br J Cancer* 2002, 86(7):1157–1161.
4. Ding Y, Cravero JD, Adrian K, Grippo P: Modeling pancreatic cancer *in vivo*: from xenograft and carcinogen-induced systems to genetically engineered mice. *Pancreas* 2010, 39(3):283–292.
5. Voskoglou-Nomikos T, Pater JL, Seymour L: Clinical predictive value of the *in vitro* cell line, human xenograft, and mouse allograft preclinical cancer models. *Clin Cancer Res* 2003, 9(11):4227–4239.
6. Femia AP, Caderni G: Rodent models of colon carcinogenesis for the study of chemopreventive activity of natural products. *Planta Med* 2008, 74(13):1602–1607.
7. Bruce WR: Counterpoint: From animal models to prevention of colon cancer. Criteria for proceeding from preclinical studies and choice of models for prevention studies. *Cancer Epidemiol Biomarkers Prev* 2003, 12(5):401–404.
8. Reddy BS: Studies with the azoxymethane-rat preclinical model for assessing colon tumor development and chemoprevention. *Environ Mol Mutagen* 2004, 44(1):26–35.
9. Reddy BS, Maeura Y: Tumor promotion by dietary fat in azoxymethane-induced colon carcinogenesis in female F344 rats: influence of amount and source of dietary fat. *J Natl Cancer Inst* 1984, 72(3):745–750.
10. Tanaka T, Kohno H, Suzuki R, Yamada Y, Sugie S, Mori H: A novel inflammation-related mouse colon carcinogenesis model induced by azoxymethane and dextran sodium sulfate. *Cancer Sci* 2003, 94(11):965–973.
11. Yoshimi K, Tanaka T, Takizawa A, Kato M, Hirabayashi M, Mashimo T, Serikawa T, Kuramoto T: Enhanced colitis-associated colon carcinogenesis in a novel Apc mutant rat. *Cancer Sci* 2009, 100(11):2022–2027.
12. Carlsson G, Gullberg B, Hafstrom L: Estimation of liver tumor volume using different formulas - an experimental study in rats. *J Cancer Res Clin Oncol* 1983, 105(1):20–23.
13. Hanahan D, Weinberg RA: The hallmarks of cancer. *Cell* 2000, 100(1):57–70.
14. Ogawa K, Mukai T, Kawai K, Takamura N, Hanaoka H, Hashimoto K, Shiba K, Mori H, Saji H: Usefulness of competitive inhibitors of protein binding for

improving the pharmacokinetics of 186Re-MAG3-conjugated bisphosphonate (186Re-MAG3-HBP), an agent for treatment of painful bone metastases. *Eur J Nucl Med Mol Imaging* 2009, 36(1):115–121.
15. Thomas DM, Zalcberg JR: 5-fluorouracil: a pharmacological paradigm in the use of cytotoxics. *Clin Exp Pharmacol Physiol* 1998, 25(11):887–895.
16. Cao S, Rustum YM: Synergistic antitumor activity of irinotecan in combination with 5-fluorouracil in rats bearing advanced colorectal cancer: role of drug sequence and dose. *Cancer Res* 2000, 60(14):3717–3721.
17. Salonga D, Danenberg KD, Johnson M, Metzger R, Groshen S, Tsao-Wei DD, Lenz HJ, Leichman CG, Leichman L, Diasio RB, *et al*: Colorectal tumors responding to 5-fluorouracil have low gene expression levels of dihydropyrimidine dehydrogenase, thymidylate synthase, and thymidine phosphorylase. *Clin Cancer Res* 2000, 6(4):1322–1327.

doi:10.1186/1471-2407-12-448
Cite this article as: Yoshimi *et al.*: Use of a chemically induced-colon carcinogenesis-prone *Apc*-mutant rat in a chemotherapeutic bioassay. *BMC Cancer* 2012 12:448.

Carcinogenesis vol.33 no.12 pp.2499–2506, 2012
doi:10.1093/carcin/bgs303
Advance Access publication October 2, 2012

Preventive effects of branched-chain amino acid supplementation on the spontaneous development of hepatic preneoplastic lesions in C57BL/KsJ-*db/db* obese mice

Daishi Terakura[1], Masahito Shimizu[1,*], Junpei Iwasa[1], Atsushi Baba[1], Takahiro Kochi[1], Tomohiko Ohno[1], Masaya Kubota[1], Yohei Shirakami[1], Makoto Shiraki[1], Koji Takai[1], Hisashi Tsurumi[1], Takuji Tanaka[2] and Hisataka Moriwaki[1]

[1]Department of Gastroenterology, Gifu University Graduate School of Medicine, Gifu 501–1194, Japan and [2]The Tohkai Cytopathology Institute: Cancer Research and Prevention (TCI-CaRP), Gifu 500–8285, Japan

[*]To whom correspondence should be addressed. Masahito Shimizu, Department of Gastroenterology, Gifu University Graduate School of Medicine, 1-1 Yanagido, Gifu 501–1194, Japan. Tel: +81 58 230 6313; Fax: +81 58 230 6310;
Email: shimim-gif@umin.ac.jp

Obesity and its associated disorders, such as non-alcoholic steatohepatitis, increase the risk of hepatocellular carcinoma. Branched-chain amino acids (BCAA), which improve protein malnutrition in patients with liver cirrhosis, reduce the risk of hepatocellular carcinoma in these patients with obesity. In the present study, the effects of BCAA supplementation on the spontaneous development of hepatic premalignant lesions, foci of cellular alteration, in *db/db* obese mice were examined. Male *db/db* mice were given a basal diet containing 3.0% of either BCAA or casein, a nitrogen-content-matched control of BCAA, for 36 weeks. On killing the mice, supplementation with BCAA significantly inhibited the development of foci of cellular alteration when compared with casein supplementation by inhibiting cell proliferation, but inducing apoptosis. BCAA supplementation increased the expression levels of peroxisome proliferator-activated receptor-γ, $p21^{CIP1}$ and $p27^{KIP1}$ messenger RNA and decreased the levels of c-*fos* and cyclin D1 mRNA in the liver. BCAA supplementation also reduced both the amount of hepatic triglyceride accumulation and the expression of interleukin (IL)-6, IL-1β, IL-18 and tumor necrosis factor-α mRNA in the liver. Increased macrophage infiltration was inhibited and the expression of IL-6, TNF-α, and monocyte chemoattractant protein-1 mRNA in the white adipose tissue were each decreased by BCAA supplementation. BCAA supplementation also reduced adipocyte size while increasing the expression of peroxisome proliferator-activated receptor-α, peroxisome proliferator-activated receptor-γ and adiponectin mRNA in the white adipose tissue compared with casein supplementation. These findings indicate that BCAA supplementation inhibits the early phase of obesity-related liver tumorigenesis by attenuating chronic inflammation in both the liver and white adipose tissue. BCAA supplementation may be useful in the chemoprevention of liver tumorigenesis in obese individuals.

Introduction

Obesity is a serious health problem worldwide since it often causes a number of medical disorders, including metabolic syndrome and type 2 diabetes mellitus. Recent evidence also indicates that obesity and its related metabolic abnormalities are associated with an increased risk of developing hepatocellular carcinoma (HCC (1–5)). Non-alcoholic fatty liver disease (NAFLD) is a hepatic manifestation of metabolic syndrome and a subset of patients with this disease can progress to non-alcoholic steatohepatitis (NASH), which involves the risk of developing chronic hepatitis, cirrhosis and HCC (6–8). Obesity and diabetes mellitus have been shown to increase the risk of developing HCC also in patients with viral hepatitis (3,5). A state of chronic inflammation caused by insulin resistance and hepatic steatosis is considered to play a critical role in the development of HCC in several obesity-related pathophysiological conditions (2,6–10). Therefore, obese patients, especially those with complications of NASH or chronic viral hepatitis, are at high risk for developing HCC, and targeting chronic inflammation might be an effective strategy for preventing obesity-related liver carcinogenesis (11).

Branched-chain amino acids (BCAA), which are a group of three essential amino acids comprising valine, leucine and isoleucine, are used clinically to improve protein malnutrition in patients with liver cirrhosis (12,13). Oral supplementation with BCAA prevents progressive hepatic failure and improves event-free survival in patients with chronic liver diseases (14,15). Moreover, a multicenter, randomized controlled trial has reported that long-term oral BCAA supplementation reduced the risk of developing HCC in patients with chronic viral hepatitis; however, the effect was evident only in the patients who are obese (3). The results seen in that clinical trial are considered to be associated with the improvement of insulin resistance achieved by BCAA supplementation (13,16). In fact, BCAA supplementation inhibited the development of carcinogen-induced liver and colorectal carcinogenesis in obese mice by improving insulin resistance (17,18). Treatment with BCAA also suppressed insulin-induced proliferation of HCC cells by antagonizing the anti-apoptotic function of insulin (19).

In addition to improving protein malnutrition and glucose metabolism, BCAA supplementation has been reported to reduce lipid deposition in the liver in recent rodent studies (17,20). Supplementation with BCAA also retarded excess weight gain and reduced epididymal white adipose tissue (WAT) weight in mice that fed a high-fat diet (20). Because chronic low-grade systemic inflammation produced by excess lipid storage in WAT and liver is involved in both the development of NASH and the obesity-related liver tumorigenesis (2,6–10), BCAA supplementation may prevent the development of liver neoplasms in obese mice by reducing excess fat accumulation in WAT and by improving liver steatosis, thereby attenuating inflammation in these organs.

The spontaneous development of hepatic preneoplastic lesions, foci of cellular alteration (FCA), have been previously reported to be enhanced in obese and diabetic C57BL/KsJ-*db/db* (*db/db*) mice, when compared with C57B6 or C57BL/KsJ-+/+ mice, genetic controls for *db/db* mice (17). In the present study, we examined the effects of BCAA supplementation on the spontaneous development of FCA in *db/db* mice while focusing on the attenuation of inflammation in both the liver and the WAT. In addition, we investigated whether BCAA supplementation alters adipocyte size and the expression of peroxisome proliferator-activated receptor (PPAR)-α, PPAR-γ and adiponectin, which are key regulators of inflammatory signaling in obese adipose tissue (21–25), in the WAT of *db/db* mice.

Abbreviations: BCAA, branched-chain amino acids; FCA, foci of cellular alteration; HCC, hepatocellular carcinoma; H&E, hematoxylin and eosin; IL: interleukin; NAFLD, non-alcoholic fatty liver disease; NASH, non-alcoholic steatohepatitis; PCNA, proliferating cell nuclear antigen; PPAR, peroxisome proliferator-activated receptor; RT–PCR, reverse transcription–PCR; SEM, standard error mean; TNF-α, tumor necrosis factor-α; WAT, white adipose tissue.

Materials and methods

Mice and diets

Male *db/db* mice (4 weeks old) were obtained from Japan SLC (Shizuoka, Japan) and humanely maintained at Gifu University Life Science Research Center in accordance with Institutional Animal Care Guidelines. BCAA and casein were obtained from Ajinomoto (Tokyo, Japan). The BCAA composition (2:1:1.2 = leucine:isoleucine:valine) was set at the clinical dosage used for the treatment of decompensated liver cirrhosis in Japan (3,14).

Experimental procedure

The experimental protocol was approved by the Institutional Committee of Animal Experiments of Gifu University. At 5 weeks of age, a total of 10 *db/db* mice were divided into two groups. The mice in Group 2 ($n = 5$) were given a basal diet (CRF-1, Oriental Yeast, Tokyo, Japan) supplemented with 3.0% BCAA (w/w) through the end of the experiment, whereas the mice in Group 1 ($n = 5$) were given a basal diet supplemented with 3.0% casein (w/w) that served as a nitrogen-content-matched control for the BCAA-treated group. At 41 weeks of age (after 36 weeks of supplementation with the experimental diet), all of the mice were killed using CO_2 asphyxiation and the development of FCA was analyzed.

Histopathology and measurement of adipocyte size

Maximum sagittal sections of each liver lobe (six sublobes) and WAT obtained from the periorchis were used for histological examination. The tissue specimens were fixed in 10% buffered formaldehyde and then embedded in paraffin. The sections (4 μm thick) were cut from the tissue blocks and stained with hematoxylin and eosin (H&E). The presence of FCA, which are phenotypically altered hepatocytes showing swollen and basophilic cytoplasm and hyperchromatic nuclei, was determined according to the criteria described previously (26). The multiplicity of the FCA was assessed on a per unit area basis (per cm^2). Fatty metamorphosis (% of fatty degeneration) was determined on the H&E-stained liver section using the BZ-Analyzer-II software (KEYENCE, Osaka, Japan (27)).

To evaluate adipocyte size, 10 adipocytes from each stained section (a total of 50 adipocytes) in each group were analyzed using a fluorescence microscope BZ-9000 (KEYENCE). Adipocyte size was measured and averaged using the BZ-Analyzer-II (KEYENCE). The unit of mean adipocyte size was square micrometers (μm^2).

Immunohistochemical analysis of proliferating cell nuclear antigen and F4/80

Immunohistochemical staining of proliferating cell nuclear antigen (PCNA), a G_1-to-S phase marker, was performed to estimate the cell proliferative activity of FCA using an anti-PCNA antibody (1:100; Santa Cruz Biotechnology, Santa Cruz, CA, USA). On the PCNA-immunostained sections, the cells with intensively reacted nuclei were considered to be positive for PCNA, and the indices (%) were calculated in 20 FCA randomly selected from each group (28).

Immunohistochemical staining to detect F4/80, a mature macrophage marker, was also performed to estimate the presence of macrophage infiltration in the WAT. After endogenous peroxidase activity was blocked with H_2O_2, the sections were incubated with a F4/80 primary antibody (1:50; AbD Serotec, Oxford, UK) for 30 min at 37°C. Subsequently, the sections were incubated with biotinylated secondary antibodies against the primary antibodies (Dako, Carpinteria, CA, USA) and then incubated with avidin-coupled peroxidase. The sections were then developed with 3,3′-diaminobenzidine using Dako Liquid DAB Substrate-Chromogen System (Dako) and counterstained with hematoxylin.

Hepatic lipid analysis

Approximately 200 mg of frozen liver was homogenized, and the lipids were extracted using a chloroform:methanol (2:1 v/v) solution, as described by Folch *et al.* (29). The levels of triglycerides in the livers of the mice were measured using the triglyceride E-test kit (Wako Pure Chemical, Osaka, Japan) according to the manufacturer's protocol (17).

RNA extraction and quantitative real-time reverse transcription–PCR analysis

Total RNA was isolated from the livers and adipose tissues of the mice using the RNeasy Mini Kit and RNeasy Lipid Tissue Mini Kit (Qiagen, Hilden, Germany), respectively. Total RNA (1 μg) was used for the synthesis of the first strand of complementary DNA using the SuperScript III First-Strand Synthesis System (Invitrogen, Carlsbad, CA, USA). Quantitative real-time reverse transcription (RT)-PCR was performed using specific primer sets that amplify PCNA, c-*fos*, interleukin (IL)-6, IL-1β, IL-18, tumor necrosis factor-α (TNF-α), monocyte chemoattractant protein-1 (MCP-1), adiponectin, PPAR-α, PPAR-γ, Bax, Bcl-2, $p21^{CIP1}$, $p27^{KIP1}$, cyclin D1 and β-actin genes. The sequences of these primers, which are obtained from the PrimerBank (http://pga.mgh.harvard.edu/primerbank/), are given in Table I. Each sample was analyzed on a LightCycler 1.0 (Roche Diagnostics, GmbH, Mannheim, Germany) with SYBR Premix Ex Taq (TaKaRa Bio, Shiga, Japan). The expression level of each gene was normalized to the β-actin expression level using the standard curve method (17).

Statistical analysis

All data were expressed as the mean ± the standard error mean (SEM). Differences between the two groups were analyzed using Student's *t*-test. All analyses were conducted using JMP 8.0 (SAS Institute Inc., Cary, NC, USA). Values with $P < 0.05$ were considered to be significant.

Table I. Primer sequences

Gene	Primer sequence	
PCNA	F	5′-TTTGAGGCACGCCTGATCC-3′
	R	5′-GGAGACGTGAGACGAGTCCAT-3′
c-fos	F	5'-CGGGTTTCAACGCCGACTA-3'
	R	5′-TTGGCACTAGAGACGGACAGA-3′
IL-6	F	5′-CTGCAAGAGACTTCCATCCAG-3′
	R	5-AGTGGTATAGACAGGTCTGTTGG-3′
IL-1β	F	5′-GCAACTGTTCCTGAACTCAACT-3′
	R	5-ATCTTTTGGGGTCCGTCAACT-3′
IL-18	F	5′-GTGAACCCCAGACCAGACTG-3′
	R	5′-CCTGGAACACGTTTCTGAAAGA-3′
TNF-α	F	5′-CAGGCGGTGCCTATGTCTC-3′
	R	5′-CGATCACCCCGAAGTTCAGTAG-3′
adiponectin	F	5′-TGTTCCTCTTAATCCTGCCCA-3′
	R	5′-CCAACCTGCACAAGTTCCCTT-3′
PPAR-α	F	5′-AGAGCCCCATCTGTCCTCTC-3′
	R	5′-ACTGGTAGTCTGCAAAACCAAA-3′
PPAR-γ	F	5′-TCGCTGATGCACTGCCTATG-3′
	R	5′-GAGAGGTCCACAGAGCTGATT-3′
MCP-1	F	5′-TTAAAAACCTGGATCGGAACCAA-3′
	R	5′-GCATTAGCTTCAGATTTACGGGT-3′
Bax	F	5′-AGACAGGGGCCTTTTTGCTAC-3′
	R	5′-AATTCGCCGGAGACACTCG-3′
Bcl-2	F	5′-ATGCCTTTGTGGAACTATATGGC-3′
	R	5′-GGTATGCACCCAGAGTGATGC-3′
$p21^{CIP1}$	F	5′-CCTGGTGATGTCCGACCTG-3′
	R	5′-CCATGAGCGCATCGCAATC-3′
$p27^{KIP1}$	F	5′-TCAAACGTGAGAGTGTCTAACG-3′
	R	5′-CCGGGCCGAAGAGATTTCTG-3′
Cyclin D1	F	5′-GCGTACCCTGACACCAATCTC-3′
	R	5′-ACTTGAAGTAAGATACGGAGGGC-3′
β-actin	F	5′-GGCTGTATTCCCCTCCATCG-3′
	R	5′-CCAGTTGGTAACAATGCCATGT-3′

Results

General observations

Body, liver, kidney and fat (WAT of the periorchis and retroperitoneum) weights and hepatic triglyceride levels of the two groups measured at the end of the study are listed in Table II. The mean liver weight and mean level of triglycerides in the livers of the mice in the BCAA supplementation group were found to be significantly less than those in the mice in the casein-treated group ($P < 0.05$). BCAA supplementation also improved macrovesicular steatosis, which was observed in the casein-fed mice ($P < 0.05$, Figure 1A), suggesting that BCAA supplementation inhibits hepatomegaly by improving the accumulation of lipids in the liver. Other measurements did not differ significantly between the two groups. All of the mice remained healthy, and no clinical signs indicating toxicity of BCAA were observed during the experiment. Histopathologically, there were no

Table II. Body, liver, kidney and fat weights and hepatic triglyceride levels of the experimental mice

Treatment	No. of mice	Body wt (g)	Relative wt (g/100 g body wt) of			Hepatic triglyceride (mg/100 mg liver tissue)
			Liver	Kidney	Fat[a]	
Casein	5	67.9±7.9[b]	7.1±1.5	0.9±0.1	9.1±2.1	13.9±2.8
BCAA	5	68.4±2.7	5.1±0.6[c]	0.9±0.1	11.0±2.5	6.8±4.4c

[a]White adipose tissue of the periorchis and retroperitoneum.
[b]Mean ± SEM.
[c]$P < 0.05$.